ACID DOPED POLYBENZIMIDAZOLE MEMBRANES FOR HIGH TEMPERATURE PROTON EXCHANGE MEMBRANE FUEL CELLS

A THESIS SUBMITTED TO
THE GRADUATE SCHOOL OF NATURAL AND APPLIED SCIENCES
OF
MIDDLE EAST TECHNICAL UNIVERSITY

BY

AHMET ÖZGÜR YURDAKUL

IN PARTIAL FULFILLMENTS OF THE REQUIREMENTS
FOR
THE DEGREE OF MASTER OF SCIENCE
IN
CHEMICAL ENGINEERING

JULY 2007

Approval of the Graduate School of Natural and Applied Sciences

_____

Prof. Canan Özgen
Director

I certify that this thesis satisfies all the requirements as a thesis for the degree of Master of Science.

_____

Prof. Nurcan Baç
Head of Department

This is to certify that we have read this thesis and that in our opinion it is fully adequate, in scope and quality, as a thesis for the degree of Master of Science.

_____	_____
Prof. İnci Eroğlu Co-supervisor	Prof. Nurcan Baç Supervisor

Examining Committee Members

Prof. Dr. Ülkü Yılmazer	(METU, CHE)	_____
Prof. Dr. Nurcan Baç	(METU, CHE)	_____
Prof. Dr. İnci Eroğlu	(METU, CHE)	_____
Asst. Prof. Dr. Mehmet Sankır	(TOBB, CHEM)	_____
Instr. Dr. Burcu Akata Kurç	(METU, TVSHE)	_____

I hereby declare that all information in this document has been obtained and presented in accordance with academic rules and ethical conduct. I also declare that, as required by these rules and conduct, I have fully cited and referenced all materials and results that are not original to this work.

Name, Last name: Ahmet Özgür Yurdakul

Signature:

ABSTRACT

ACID DOPED POLYBENZIMIDAZOLE MEMBRANES FOR HIGH TEMPERATURE PROTON EXCHANGE MEMBRANE FUEL CELLS

Yurdakul, Ahmet Özgür
MS., Department of Chemical Engineering
Supervisor: Prof. Nurcan Baç
Co-supervisor: Prof. İnci Eroğlu

July 2007, 73 pages

A great deal of research on the membrane for proton exchange membrane (PEM) fuel cells has been recently focused on developing alternates with high performance and durability at high temperatures. Phosphoric acid doped polybenzimidazole membranes are one of the most successful ones among the high temperature membranes developed up to now. In these membranes, the polybenzimidazole (PBI) polymer with high mechanical, thermal and oxidative properties is used as a matrix, and phosphoric acid is doped in this matrix to allow proton transfer. When the polymer membrane is doped with high levels of acid, the performance of membrane becomes comparable with that of Nafion®. PBI membrane is also much less dependent on the humidity level of reactants compared with Nafion® which permits fuel cell operation without reactant humidification.

In this study, phosphoric acid doped membranes were developed for PEM fuel cells. First, the polymer was synthesized via a one stage solution polymerization method. Then, the characterization of synthesized polymer was performed by the analysis of infrared spectra, X-Ray diffraction, NMR spectra,

thermogravimetric analysis and viscosity measurement. Thereafter, membranes were prepared by a solution casting method with Dimethylacetamide (DMAc) as the solvent, and they were doped with acid by immersing them into the phosphoric acid solutions at different concentrations. Finally, the characterization of acid doped membranes was performed by thermogravimetric analysis, mechanical tests and conductivity measurements.

The intrinsic viscosity measurements of synthesized polymer were performed via a dilute solution viscosity technique using an Ubbelohde viscometer. The highest intrinsic viscosity was measured as 2.1 dl/g (dl = 100ml) in sulphuric acid solution at 30°C, and the average molecular weight was calculated as 126,000 using the Mark-Houwink equation.

5 wt % PBI polymer solutions were prepared by dissolving the polymer in DMAc/LiCl solvent system at 70°C with 2 hrs of stirring in an ultrasonic bath. The polymer solutions were used for the membrane casting. The thinnest membranes were obtained as 30-40 μm. The prepared membranes were immersed into the phosphoric acid solutions of 11, 13, 14 and 14.7 M. The acid doping levels were obtained as 6, 8, 10 and 11 moles H_3PO_4/polymer repeat unit.

The TGA of the acid doped membranes up to 200°C in air indicated that there was no permanent weight loss caused by decomposition. The tension tests were performed at ambient temperature, and the highest and lowest stresses at break were obtained as 23 MPa and 11 MPa for the membranes having intrinsic viscosity of 2.1 dl/g with acid doping levels of 6 moles and 11 moles, respectively. The conductivity measurements were performed in a humidity chamber at 110, 130 and 150°C in both dry and humid air. The highest conductivity was obtained as 0.12 S/cm for the 11 mole acid doped membrane at 150°C and 33% RH. Moreover, the conductivity value for the same membrane was measured as 0.053 S/cm at 150°C in dry air which was a promising level for a high temperature fuel cell operation without humidity.

Keywords: acid doped polybenzimidazole, synthesis, membrane characterization

ÖZ

YÜKSEK SICAKLIKTA ÇALIŞAN PROTON GEÇİRGEN ZARLI YAKIT PİLLERİ İÇİN ASİT YÜKLÜ POLİBENZİMİDAZOL ZARLAR

Yurdakul, Ahmet Özgür
Y. Lisans, Kimya Mühendisliği Bölümü
Tez danışmanı: Prof. Nurcan Baç
Yardımcı tez danışmanı: Prof. İnci Eroğlu

Temmuz 2007, 73 sayfa

Son zamanlarda proton iletken zarlı (PEM) yakıt pillerinde kullanılan zarlar üzerine yapılan çalışmaların büyük bir kısmı yüksek sıcaklıkta yüksek performans ve dayanıklılık gösterebilen alternatifler üzerine yoğunlaşmıştır. Şimdiye kadar geliştirilen yüksek sıcaklığa dayanıklı tüm zarlar arasında en başarılı olanlardan bir tanesi de fosforik asit yüklü polibenzimidazollerdir. Bu zarın iskeletini yüksek mekanik, termal ve oksidatif dayanıklılığa sahip bir polimer olan polibenzimidazol (PBI) oluşturmaktadır. Bu yapıya fosforik asit yüklendiğinde ise zar, proton iletken hale gelmektedir. Bu zarlar yüksek asit yüklerinde, Nafyon zarla karşılaştılabilecek seviyede proton iletkenliğe sahiptir. İletkenliğinin ortamdaki neme olan bağımlılığı Nafyon'a göre çok daha az olduğundan, bu özellik PEM yakıt pillerinin, gazların nemlendirilmesine gerek kalmadan çalıştırılmasını sağlaması açışından önemlidir.

Bu çalışmada, PEM yakıt pilleri için asit yüklü polibenzimidazol zarlar geliştirilmiştir. İlk önce, polimer, tek aşamalı bir solüsyon polimerizasyon yöntemi kullanılarak sentezlenmiştir. Sentezlenen polimerlerin kızılötesi, X-ışını, NMR,

sıcaklık-kütle analizi ve viskozite ölçümleri ile nitelikleri saptanmıştır. Sonrasında bu polimerlerden, çözücü olarak Dimetilasetamit (DMAc) kullanıldığı solüsyon dökme yöntemiyle zarlar üretilmiştir. Bu zarlar değişik derişimdeki fosforik asit çözeltileri içinde asit yüklenmesi için bekletilmiştir. Son olarak, asitle yüklenmiş zarların sıcaklık-kütle, mekanik dayanıklılık ve iletkenlik testleri yapılmıştır.

Sentezlenen polimerlerin akışmazlık testleri, sülfürik asitte çözülmüş değişik derişimdeki polimer çözeltisinin, bir Ubbelohde viskometre kullanılarak, 30°C'deki akma süresinin ölçülmesiyle yapılmıştır. En yüksek içsel viskozite değeri 2.1 dl/g olarak ölçülmüştür, buradan da Mark-Houwink denklemi kullanlılarak polimerin ortalama molekül ağırlığı 126.000 olarak hesaplanmıştır.

Ağırlıkça % 5 PBI polimer çözeltileri, polimerin ağırlıkça %1 LiCl içeren DMAc içinde 70°C'de, bir ultrasonik karıştırıcı ile, yaklaşık 2 saat karıştırılarak hazırlanmıştır. Bu çözeltiler zar dökme için kullanılmıştır. Elde edilen zarlar, en ince 30-40 μm civarın kalınlıkta olmuştur. Hazırlanan zarlar 11, 13, 14 ve 14,7 M'lık fosforik asit çözeltileri içinde bekletilmiştir. Elde edilen zarların asit yükleri, polimer birimi başına sırasıyla 6, 8, 10 ve 11 mol asit olarak hesaplanmıştır.

200°C'ye kadar yapılan sıcaklık-kütle testleri, zarların bu sıcaklığa kadar herhangi bir kalıcı ağırlık kaybına ya da bozulmaya uğramadığını göstermiştir. Oda koşullarında yapılan çekme testlerinden (Çekme testleri için 2.1 dl/g "intrinsic viscosity" değerine sahip polimer zarlar kullanılmıştır.) elde edilen sonuçlara göre, en yüksek ve en düşük dayanıklılığa sahip olanlar, sırasıyla 23 MPa'lık çekme dayanıklılığı ile 6 mol asit yüklü ve 11 MPa'lık çekme dayanıklılığı ile 11 mol asit yüklü zarlar olmuştur. İletkenlik testleri için bir nem kabı dizayn edilmiştir ve testler bu kap ile 110, 130 ve 150°C'de hem nemli hem de nemsiz ortamda yapılmıştır. En yüksek proton ilentkenlik değeri, 11 mol asit yüklü zar için 150°C ve %33 nemli ortamda 0.12 S/cm olarak elde edilmiştir. Ayrıca aynı zar için aynı sıcaklıkta ama kuru ortamda iletkenlik değeri 0.053 S/cm olarak ölçülmüştür ve bu sonuç yüksek sıcaklıkta çalışan PEM yakıt pillerinin nemlendirme ihtiyacı olmadan çalıştırılması konusunda umut verici bir sonuç olmuştur.

Anahtar kelimeler: asit yüklü polibenzimidazol zar, sentez, zar niteliklendirmesi

To My Family

ACKNOWLEDGMENTS

I would like to thank my supervisor Prof. Nurcan Baç and my co-supervisor Prof. İnci Eroğlu for giving me the chance of participating in their fuel cell research group for my master study. I am grateful for being a schoolarship holder in their project from Tübitak.

I also thank Assoc. Head Göknur Bayram and Prof. Gürkan Karakaş for their help in the polymer issue. I always consulted them comfortably whenever I had a question about the polymer synthesis and characterization.

I acknowledge Prof. Ali Çulfaz and his co-workers for their help in X-Ray analysis.

I thank Gültekin Akay and Serdar Erkan for sharing his knowledge and ideas with me. I also thank Berker Fıçıcılar for his help in computers.

I am very glad for the help of the departmental staff of laboratory and workshop. I never met with any rejection of my intensive requests. They always patiently dealt with my demands.

I am indebted to Tübitak for their financially supporting this study belonging to project 104M364.

TABLE OF CONTENTS

LIST OF TABLES

LIST OF FIGURES

LIST OF SYMBOLS

Abbreviations

AFC: alkaline fuel cell

BI: benzimidazole

DAB: diaminobenzidine

DAB.4HCl.2H_2O: diaminobenzidine tetrahydrochloride

DI: de-ionized

DMAc: N,N-dimethylacetamide

EIS: electrochemical impedance spectroscopy

FC: fuel cell

FTIR: Fourier transform infrared

GDE: gas diffusion electrodes

GDL: gas diffusion layer

GFC: gas flow channel

IPA: isophthalic acid

IR: infrared

MEA: electrode assembly

MCFC: molten carbonate fuel cell

mPBI: m-polybenzimidazole (poly [2,2'-(m-phenylene)-5,5'-bibenzimidazole])

NMR: nuclear magnetic resonance

PAAM: polyacrylamide

PAFC: phosphoric acid fuel cell

PBI: polybenzimidazole

PEI: polyetherimide

PEEK: polyetheretherketone

PEK: polyetherketone

PEM: polymer electrolyte membrane

PEO: polyethylene oxides

PEMFC: proton exchange (polymer electrolyte) membrane fuel cell

PES: polyethersulphone

PFSA: perflorosulfonic acid

PI: polyimide

PPQ: polyphenyquinoxaline

PPA: polyphosphoric acid

PPS: polyphenylene sulphide

PS: polysulphone

PVA: polyvinyl acetate

ref: reference state

RH: relative humidity

SOFC: solid oxide fuel cell

TGA: thermogravimetric analysis

Symbols

a_c: catalyst specific area [cm^2/mg]

A: pre-exponential factor

c: the concentration level in the viscometer [gr/dl]

D: distance between inner electrodes (cm)

E: the theoretical cell potential [V]

E_a: activation energy for proton transfer [J/mol]

E_c: activation energy for O_2 reduction on the catalyst [J/mol]

E_{cell}: cell potential [V]

E_{loss}: potential losses [V]

F: the Faraday constant = 96,485 C/mol

i: current density [A/cm^2]

i_0: exchange current density [A/cm^2 Pt]

i_L: limiting current density [A/cm^2]

l_m: length of membrane (cm)

L_c: catalyst loading [mg Pt/cm^2]

M_w: molecular weight [gr/mol]

M_w^{av} : average molecular weight [gr/mol]

n: # of electrons per molecule of H_2

P: gas permeability of membrane [$mol.m.m^{-2}.s^{-1}.Pa^{-1}$]

P_{air}: partial pressure of dry air in the chamber [bar]

P_r: reactant partial pressure [kPa]

P_T: total pressure in the chamber which is read from the manometer [bar]

P_v: partial pressure of water vapor in the chamber [bar]

R: gas constant = 8.314 J/molK

R_i: total internal resistance [$\Omega.cm^2$]

R_m: resistance of membrane (Ω)

T: temperature [K]

t: the flow time of polymer solution in the viscometer [s]

t_0: the flow time through the capillary of viscometer for pure sulfuric acid [s]

t_m: thickness of membrane (μm)

T_g: glass transition temperature [°C]

T_{op}: operating temperature [°C]

w_m: width of membrane (mm)

W_{el}: electrical work [W]

Greek letters

α: transfer coefficient [dimensionless]

ΔG_{rxn}: change in Gibbs free energy due to the electrochemical reaction [J/mol]

ΔV_{act}: activation polarization [V]

ΔV_{conc}: concentration polarization [V]

ΔV_{ohm}: ohmic losses [V]

γ: pressure coefficient (0.5 to 1.0) [dimensionless]

η: viscosity of the solution [$N.s/m^2$]

η_{inh}: inherent viscosity [dl/g]

η_{int}: intrinsic viscosity [dl/g]

η_{red}: reduced viscosity [dl/g]

η_{rel}: relative viscosity [dimensionless]

η_{sp}: specific viscosity [dimensionless]

ρ: density of solution [kg/m^3]

σ: conductivity of membrane (S/cm)

υ: kinematic viscosity [m^2/s]

CHAPTER 1

INTRODUCTION

1.1 Fuel Cells

A fuel cell (FC) is an electrochemical device which converts the energy of a reaction between a fuel and an oxidant into electrical energy and heat. It has a battery like structure which consists of an electrolyte, two electrodes, positive and negative terminals. The fuel and oxidant are externally fed to the FC, and react on two catalytic surfaces separated by the electrolyte. The ions and negative charges produced by redox reactions are carried from anode to cathode side through the electrolyte and an external circuit, respectively.

An FC converts chemical energy directly into electrical energy, which eliminates all the intermediate steps required for producing electricity from a combustion engine (The fuel is converted first into heat, then mechanical motion in a combustion engine, and a generator converts the motion into electricity.). Fuel-to-electric power efficiencies as high as 65% are likely, which gives FC's the potential to be roughly twice as efficient as the average central power station operating today [1]. The heat evolved during the exothermic reaction in the FC is also used for applications such as heating and air conditioning. Fuel-cell cogeneration systems can have overall efficiencies from fuel to electricity and heat of over 80% [1]. Beside the power efficiency, an FC has a property that the pollutant combustion products such as SO_x, CO, unburned or partially burned hydrocarbons are not emitted during the conversion process. The energy obtained from an FC is not only clean but also silent. The flexibility in size and power capacity makes FC's suitable for the systems of several watts to large scale power stations of MWs. By adjusting the feed rates in an FC, it can respond to fluctuations in energy demand during operation.

Although FC's have lots of operational benefits as mentioned above, they have some drawbacks which should be addressed or overcome. The manufacturing and operating costs for FC's are still too high to compete with other energy conversion devices. The catalyst poisoning, durability and reliability issues are also being considered.

1.1.1 Historical Development of Fuel Cells

In 1839, the first FC was developed and named as "gaseous voltaic cell" by British physicist William R. Grove [2]. His work was based on reversing electrolysis to produce electrical current. He used H_2 and O_2 as reactants, platinum foil as electrodes, and dilute sulphuric acid as electrolyte in glass tubes. He performed his experiments by using a series of cells connected with a voltmeter. In Figure 1, a battery of five cells (at the left hand side) and a voltmeter connected to the battery (at the right hand side) are shown from his paper published in 1843 [3].

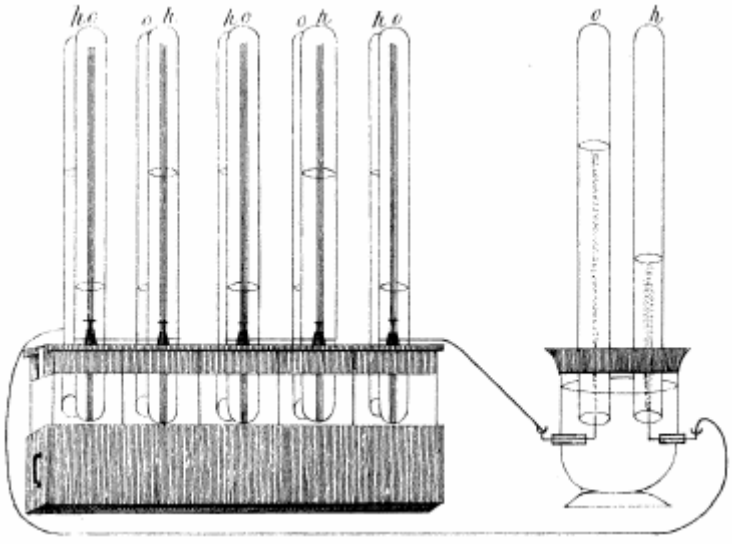

Figure 1. Grove's battery of five cells connected with a voltmeter [3]

The name “fuel cell” was coined by British chemists Ludwig Mond and his assistant German-born Charles Langer [1]. In 1889, they built an FC with a longer life time. In order to increase contact time between the reactant gasses, the electrolyte and the catalyst while obtaining the highest possible conversion, they adopted a construction shown in Figure 2. It contains a diaphragm of porous non-conducting substance impregnated with dilute sulphuric acid, covered with a thin layer of Pt or Au, and a thin layer of Pt black. The diaphragms prepared were placed side by side with non-conducting substances so as to form gas flow fields. These diaphragms were so connected that the gasses passed in contact with a number of diaphragms [4]. They obtained 21mA/cm^2 at 0.58 V from a 42 cm^2 battery they constructed.

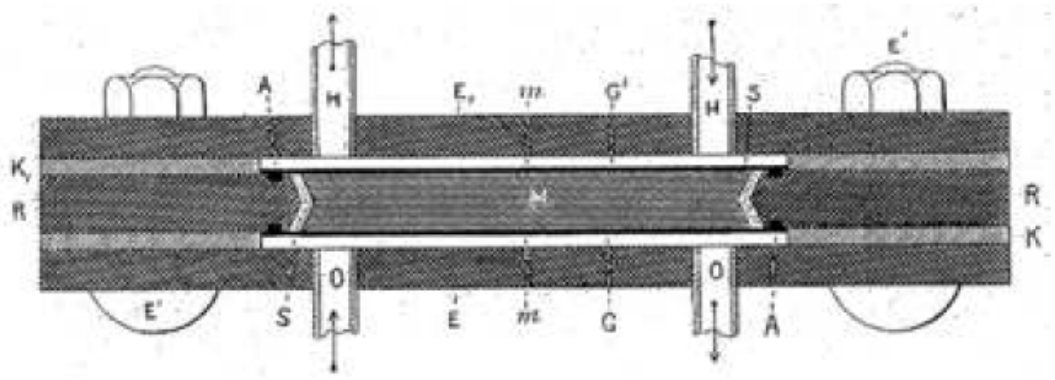

Figure 2. L. Mond’s fuel cell diagram [4]

During the early years of the 20th century, Fritz Haber and Walter H. Nernst in Germany, and Edmund Bauer in France performed experiments with fuel cells by using a solid electrolyte instead of dilute sulphuric acid, which was the electrolyte of 19th century fuel cells. British engineer Francis T. Bacon began working on FC’s in 1932, and developed a 6 kW alkaline fuel cell (AFC), which is usually considered as the first practical FC, in 1959 [5]. In his design, he replaced the platinum electrode with less expensive nickel gauze, and used alkali potassium hydroxide as electrolyte which is less corrosive to the FC parts than sulphuric acid.

In the same year, the Allis-Chalmer demonstrated a tractor powered by a 15 kW stack.

The boosting step in practical application of fuel cell technology was undertaken by the National Aeronautics and Space Administration (NASA) which was looking for a clean and safe power source for manned spaceships they developed. In 1955, a chemist in General Electric (GE), Willard Thomas Grubb, further modified the FC design by using sulphonated polystyrene ion exchange membrane as electrolyte, and this was the first polymer electrolyte membrane (PEM) FC. Another GE chemist, Leonard Niedrach, devised a way of loading Pt onto this membrane. The PEMFC developed by GE researchers was used in the Gemini Program by NASA in early 1960s. In the Apollo space program, Apollo, FC's built by Pratt and Whitney Aircraft based on a license taken on Bacon's patents were used to generate electricity for life support, guidance and communications [6].

Although the FC technology was used in space programs, there was little interest on FC's for earth applications till 1970s. The oil crisis in 1973 triggered the researches on alternative power sources to reduce dependence on petroleum import. A number of companies and government organizations such as Ballard Power systems Inc. from Canada; United Technologies Corp. (UTC), Plug Power, Analytic power, GE, Union Carbide, Exxon/Ashthom, Ford, Energy Research Corp., M-C Power Corp. from the USA; Toyota, Mazda, Honda, Toshiba, Hitachi Ltd., Ishikawajima-Harima Heavy Industries Ltd., Fuji Electric, Mitsubishi Electric Corp. from Japan; H-Power from UK; Siemens, Deutsche Aerospace, Daimler-Benz from Germany; ELENCO from Belgium; CGE from France; DeNora, Ansaldo Energia from Italy and etc. began to do research on overcoming the drawbacks of FC's so as to commercialize them as alternate to petroleum based energy sources. In 1991, a 200 kW phosphoric acid fuel cell (PAFC) was introduced by UTC which was the first commercialized FC technology. The first FC powered bus was launched by Ballard Inc. in 1993. Honda, Mazda, Nissan and Daimler-Benz were involved in developing cars powered by Ballard's FC's. At the beginning of 21st century, many

electrical equipment manufacturers began to produce power generation equipment based on FC technology.

In the recent years, FC's have been installed in hospitals and schools, and many of the major automotive companies have unveiled prototype FC powered cars. Trails of FC powered buses have taken place in Chicago and Vancouver with other cities in North America and Europe looking to take delivery of these vehicles in the near future.

1.1.2 Types of Fuel Cells

Various types of FC's have been developed. They are generally classified based on the electrolyte used which determines the operating temperature (T_{op}) and the kind of fuel that can be applied. According to the characteristics of the electrolyte, FC's are divided into five types: PAFC, Molten Carbonate fuel cell (MCFC), solid oxide fuel cell (SOFC), AFC, and PEMFC.

PAFC's use concentrated orthophosphoric acid (~100%) as electrolyte transporting protons from anode to cathode side. The acid is kept usually in a matrix of SiC. The T_{op} is 170-200°C. Both the anode and cathode catalysts are platinum. The reactions taking place are given in Equation (1.1) and (1.2);

$$H_2 \rightarrow 2\,H^+ + 2\,e^- \qquad \text{anode side} \qquad (1.1)$$

$$\tfrac{1}{2}\,O_2 + 2\,H^+ + 2\,e^- \rightarrow H_2O \qquad \text{cathode side} \qquad (1.2)$$

PAFC's are tolerant to CO in reformate fuel due to the level of operation temperature. The co-generation efficiency of electricity is about 85%, but the efficiency of electricity only is 40-45% which is the lowest one among the fuel cell types [7], so it means a larger, heavier and more expensive FC. These FC's were introduced into the market in the 1990s as 200 kW packages for stationary electricity generation by UTC, and there are hundreds of these units installed all over the world.

MCFC's use an electrolyte composed of molten carbonate salt mixture suspended in a porous, chemically inert ceramic $LiAlO_2$ matrix transporting CO_3^{-2} from cathode to anode side. The T_{op} is 600-700°C which allows non-precious

metals such as Ni to be used as the catalyst. The reactions are given in Equation (1.3) and (1.4);

$$H_2 + CO_3^{-2} \rightarrow H_2O + CO_2 + 2\ e^- \qquad \text{anode side} \qquad (1.3)$$

$$½\ O_2 + CO_2 + 2\ e^- \rightarrow CO_3^{-2} \qquad \text{cathode side} \qquad (1.4)$$

MCFC's are not prone to CO poisoning due to high T_{op}. There is a potential for the FC waste heat to be used to reform a hydrocarbon fuel such as CH_4 into H_2 by the FC itself (in-situ reforming). The efficiency of producing electricity is 45-60% [7]; when the waste heat is used, the overall efficiency can be 85%. The primary drawback of this FC technology is the durability problem. Currently, corrosion-resistant materials for components are investigating.

SOFC's use a hard, non-porous ceramic material made of zirconia and yttria as electrolyte which transports O^{-2} ions from cathode to anode side. The T_{op} is 900-1000°C that non-precious metals such as Ni can be used as the catalyst. The reactions at the anode and cathode are given in Equation (1.5) and (1.6);

$$H_2 + O^{-2} \rightarrow H_2O + 2\ e^- \qquad \text{anode side} \qquad (1.5)$$

$$½\ O_2 + 2\ e^- \rightarrow O^{-2} \qquad \text{cathode side} \qquad (1.6)$$

SOFC's are the most resistant type of FC's to CO and S. It is valid for these FC's as for MCFC's that the waste heat can be used for combined cycle steam or combined cycle gas turbines as well as internal fuel reforming. The efficiency for electric power is 50-60% and for cogeneration is 80-85% [1]. The disadvantages of this type of FC are slow start-up, thermal shield requirement to retain heat, and the durability problem. The key technical challenge is to develop low-cost materials with high durability at cell operating conditions (OC).

AFC's use a solution of KOH in water as the electrolyte that carries OH^- ions from cathode to anode side. The catalysts of anode and cathode can be non-precious materials such as Ni and NiO. The T_{op} is 50-200°C. The reactions for this type of FC are given in equations (1.7) and (1.8);

$$H_2 + 2\ OH^- \rightarrow 2\ H_2O + 2\ e^- \qquad \text{anode side} \qquad (1.7)$$

$$½\ O_2 + H_2O + 2\ e^- \rightarrow 2\ OH^- \qquad \text{cathode side} \qquad (1.8)$$

AFC's have high performance due to the fast rate of reactions. The efficiency for electrical conversion is as high as 60%. These highly efficient and reliable FC's were developed for the space programs in the 1960's. The major difficulty with AFC's is their intolerance to CO_2 even at low levels found in the atmosphere, and so it is not possible to use air as O_2 source for the cathode side as it contains CO_2.

PEMFC's use a polymer as the electrolyte which carries protons produced at the anode side to the cathode side. The T_{op} is 60-80°C for the traditional Nafion® membrane. Precious noble metals or metal composites such as Pt and Pt/Ru with carbon supports are used as the catalyst at both anode and cathode side. The reactions taking place are same as those for PAFC's;

$$H_2 \rightarrow 2\ H^+ + 2\ e^- \qquad \text{anode side} \qquad (1.1)$$

$$½\ O_2 + 2\ H^+ + 2\ e^- \rightarrow H_2O \qquad \text{cathode side} \qquad (1.2)$$

PEMFC's have an efficiency of 40-50% for electrical power generation. Because they are operated at low temperatures, the start-up is quick and less wear on system components is applied resulting in better durability; but CO poisons the Pt catalyst at low temperatures, so pure H_2 is needed. They are used for transportation purposes and portable applications, and some stationary applications. Due to their fast start-up, low sensitivity to orientation, and favorable power-to-weight ratio, they are generally thought to be suitable for portables and vehicles. The main drawbacks for these FC's are the CO poisoning issue, water and heat management, high cost, degradation and fuel storage problem.

The summary of the properties and the working principles of FC types are given in Figure 24 and Table 6 in Appendix A. Some good reviews summarize the fuel cell technology, including historical notes, types, design and configuration, benefits and limitations, future technical developments, and potential markets [8], [9], [10].

1.2 Purpose of the Research

Today's energy demand has begun to shift to the renewable energy sources due to the possibility of depletion of fossil fuels in the near future and the threat of

global warming. FC's are one of the most attractive energy conversion devices thought to be a substitute for the conventional combustion engines because of that they do not produce or emit greenhouse gases.

Among the FC types, PEMFC's have properties of low weight to power ratio and quick start-up. The reason why they have not been commercialized and mass produced yet is that they still have operating temperature limitations, short life-time, high manufacturing and operating costs, heat and water management difficulties. Intensive research on PEM's are continued to eliminate these problems. The most effort is concentrated on development of new PEM's durable to high temperature, chemically and dimensionally stable, non-sensitive to humidity, and with low cost.

Phosphoric acid doped polybenzimidazole (PBI) membranes are one of the alternatives to the conventional Nafion®. These membranes enable PEMFC's to operate at high temperatures (up to 200°C), so that the water and heat management problems for PEMFC's can be overcome, and higher percentages of impurities in the fuel can be tolerated. They can also be operated without humidification of reactant gases. They were first applied to PEMFC's by Wainright et al. in 1995 [11], and in the succeeding years, intensive research have been conducted to develop them. As acid doping level is increased, the conductivity of these membranes also increases, but due to the mechanical limitations, they are not suitable to be doped with acid at higher levels (i.e. above 6 moles of acid per polymer repeat unit). In this research, PBI polymer with high molecular weight was planned to be synthesized, so that it would be possible to obtain membranes having a high mechanical strength which would be more durable at higher acid doping levels.

In this study, synthesis and characterization of PBI polymer was performed, first. Then the membranes were prepared from the polymer by film casting method. After that, the membranes were doped with H_3PO_4 by immersing and keeping in the H_3PO_4 solutions at specific concentrations. Finally, the characterization of the membranes such as ionic conductivity and mechanical strength measurements were performed.

CHAPTER 2

LITERATURE SURVEY

2.1 Proton Exchange Membrane Fuel Cells

Recently, PEMFC's have extensively been studied because of their promising advantages such as high power density, low weight to power ratio, pollution-free operation, and all-solid construction (thus less corrosion). These studies have resulted in a multitude of PEMFC demonstrations for stationary, transportation and portable applications. In the last decade, realizing the advantages of high temperature operation of PEMFC's, the research have been intensified on the development of alternate PEM's.

2.1.1 High Temperature Operation of PEM Fuel Cells

Although PEMFC technology typically operates between 60 and 80°C due to thermal limitations of the electrolytes used, it is desirable to increase the T_{op} above 100°C. There are several technical and commercial advantages for operating PEMFC's at temperatures above 100°C: Rates of the electrochemical reactions are enhanced, water and heat managements are simplified, useful waste heat can be recovered, tolerance level to fuel impurity increases resulting in a simpler reformer producing H_2.

2.1.1.1 Effect of temperature on fuel cell thermodynamics, electrochemistry, and mass transport properties

The maximum electrical work, W_{el}, obtained from the electrochemical reaction system is defined as given in Equation (2.1),

$$W_{el} = n \times F \times E \qquad (2.1)$$

where n: # of electrons per molecule of H_2,

F: the Faraday constant,

E: the theoretical cell potential

The Equation (2.1) can be rewritten for E as Equation (2.2),

$$E = \frac{W_{el}}{nF} \tag{2.2}$$

Thermodynamically, $-W_{el}$ is equal to the change in Gibbs free energy due to the electrochemical reaction, ΔG_{rxn}. Then, E is also written as Equation (2.3),

$$E = \frac{-\Delta G_{rxn}}{nF} \tag{2.3}$$

The value of ΔG_{rxn} for the electrochemical reaction of PEMFC increases with temperature, so E decreases with increasing temperature. In Table 1, the values of E at different temperatures are given for comparison.

Table 1. E and ΔG_{rxn} values of the electrochemical reaction of PEMFC [6]

T(°C)	ΔG_{rxn}(kJ/molK)	E(V)
25	-237.34	1.230
60	-231.63	1.200
80	-228.42	1.184
100	-225.24	1.167

The cell potential, E_{cell}, is equal to the open circuit voltage (V_{OC}) reduced by potential losses, E_{loss},

$$E_{cell} = V_{OC} - E_{loss} \tag{2.4}$$

E_{loss} includes the activation polarization (ΔV_{act}), ohmic losses (ΔV_{ohm}), and concentration polarization (ΔV_{conc}),

$$E_{loss} = \Delta V_{act} + \Delta V_{ohm} + \Delta V_{conc} \tag{2.5}$$

ΔV_{act} can be written according to the Butler-Volmer Equation,

$$\Delta V_{act} = \frac{RT}{\alpha F} \ln\left(\frac{i}{i_0}\right) \tag{2.6}$$

where R: gas constant

T: temperature

α: transfer coefficient

i: current density

i_0: exchange current density

ΔV_{conc} can be written according to the Nernst Equation,

$$\Delta V_{conc} = \frac{RT}{nF} \ln\left(\frac{i_L}{i_L - i}\right) \tag{2.7}$$

where i_L: limiting current density

ΔV_{ohm} can be expressed by Ohm's law,

$$\Delta V_{ohm} = iR_i \tag{2.8}$$

where R_i: total internal resistance

Then, the Equation (2.4) is rewritten by substituting equations (2.6), (2.7) and (2.8),

$$E_{cell} = V_{OC} - \frac{RT}{\alpha F} \ln\left(\frac{i}{i_0}\right) - iR_i - \frac{RT}{nF} \ln\left(\frac{i_L}{i_L - i}\right) \tag{2.9}$$

Here, i_0 is the exchange current density (the rate at which the oxidation and reduction reactions on an electrode proceed at equilibrium), which is analogous to the rate constant in chemical reactions and expressed as follows [6],

$$i_0 = i_{0,ref} a_c L_c \left(\frac{P_r}{P_{r,ref}}\right)^{\gamma} \exp\left[-\frac{E_c}{RT}\left(1 - \frac{T}{T_{ref}}\right)\right] \tag{2.10}$$

where ref: reference state

a_c: catalyst specific area

L_c: catalyst loading

P_r: reactant partial pressure

γ: pressure coefficient (0.5 to 1.0)

E_c: activation energy for O_2 reduction on the catalyst

According to Equation (2.10), i_0 increases with increasing temperature.

In Equation (2.9), the term multiplied with the logarithmic term for activation polarization is called as Tafel slope. α is independent of temperature [6], so Tafel slope increases with temperature.

Diffusivity, D, is the determining parameter of mass transport properties of species. Beside molecular diffusion, the convectional mass transfer is proportional to D, and D increases with temperature [12].

In summary, increased temperature results in theoretical potential loss (Equation (2.3)) and a higher Tafel slope, which means a lower potential (Equation (2.9)), while higher i_0 and significantly improved species mass transfer are the results of higher T_{op}. Although, the theory does not give an exact conclusion, FC performance tests indicate that the overall effect of increasing temperature is an increase in cell performance.

2.1.1.2 Effect of temperature on tolerance of catalyst to contaminants

The fuel of PEMFC's, H_2, is not readily available, and it is usually produced by reforming. The reformate gas also includes gases other than H_2, and one of these gases, CO, has a poisoning effect on the Pt catalyst. It is adsorbed on the catalyst active sites (Equation (2.11)), and so prevents the hydrogen adsorption on these sites (Equation (2.12)) for the oxidation reaction.

$$CO + Pt \rightarrow Pt\text{-}CO \quad (2.11)$$

$$H_2 + 2\,Pt \rightarrow 2\,Pt\text{-}H \quad (2.12)$$

The adsorption of CO on Pt is due to high negative entropy, and disfavored with increasing temperature. Thermodynamically, H_2 adsorption is less exothermic than CO adsorption, so at higher temperatures, the coverage of CO on the active sites decreases, while H_2 coverage increases. It is reported in literature that the maximum tolerable amount of CO in the fuel is 10-20 ppm at 80°C and 1000 ppm at 130°C, and it increases up to 3vol % at 200°C. Zhang et al. [13] gave a good review and summarized the research in this area.

2.1.1.3 Effect of temperature on water and heat management

The water content is critical for the performance of a PEMFC operating below 100°C: insufficient water in the membrane and gas diffusion electrodes (GDE), which are named together as membrane electrode assembly (MEA), decreases the proton conductivity and increases the internal cell resistance, while excessive water through the MEA causes flooding which restricts reactant transport from gas flow channels (GFC) to catalyst active sites, which also decreases the performance. High temperature operation increases dehydration of membrane as Zhang et al. [13] discussed. Humidity is not critical for conductivity of high temperature membranes such as acid doped PBI as much as low temperature ones. Besides, at a temperature above 100°C, the operation involves only a single phase, water vapor, which mitigates the flooding problem.

During PEMFC operation, heat emerges as a result of exothermic reaction at the cathode, and it must be removed from the system via a cooling medium. The heat rejection at low temperatures is difficult due to small temperature difference between stack and environment, so complex cooling systems and high heat transfer area are needed. At higher temperatures, heat removal becomes much easier due to higher temperature gradient, so it results in a simplified cooling system, and smaller volume and mass fractions for cooling in the whole system. The waste heat can also be recovered which may then be used for heating and pressurizing the reactant gases, steam reforming or metal hydride storage tanks.

2.1.2 Proton Exchange Membranes

The heart of PEMFC's is the part of MEA. It consists of a polymer electrolyte at the center, with catalyst loaded gas diffusion electrode (GDE) layers for anode and cathode stuck onto both sides of it. For a typical H_2/O_2 PEMFC, H_2 reactant gas is fed to the anode side of MEA, and O_2 to the cathode. Each reactant gas coming from the gas flow channel (GFC) diffuses through the gas diffusion layer (GDL) and reaches to the active sites of the loaded catalyst. H_2 is converted into protons and electrons at the anode side, while O_2 reacts with protons and

electrons, carried from the anode to the cathode, resulting in formation of H_2O, heat and electricity. Here, the protons are transformed by the polymer membrane.

A desirable PEM must have the following properties,

- High proton conductivity ($\geq$ 0.1 S/cm)
- Good film formation
- Capable of fabrication into MEAs
- Thermal, oxidative and dimensional stability
- Adequate barrier to separate reactant gasses of each side
- Mechanical durability at the operating conditions of PEMFC (with mechanical strength of several MPa's)
- Long life-time [13]

  For portables → 2000- 5000 hrs

  For automobiles → 5000- 10000 hrs

  For stationary applications → 40000 hrs
- Low cost (<100\$/m^2)

Up to now, vast varieties of membranes have been developed for PEMFC operation by research groups in universities, institutes and companies. The membranes developed include perflorosulfonic acid (PFSA) polymers, modified PFSA polymers and their composites, modified aromatic polymers and their composites, and acid-base polymers. There are useful reviews in literature which summarize the PEM types developed [15]-[19].

PFSA membranes are composed of carbon fluorine backbone chains with perfluoro side chains containing sulfonic acid groups. These membranes are the most commonly used ones for low temperature PEMFC's and commercialized as Nafion® (DuPont), Dow® (Dow Chemical), Flemion® (Asahi Glass), and Aciplex® (Asahi Chemicals). Among these membranes, Nafion® is superior due to its high proton conductivity, good chemical and mechanical durability. Longevities up to 60,000 hr were achieved with these membranes at 80°C [18]. The shortcomings about PFSA membranes are operation at low temperatures only, high price, high fuel crossover, intensive water management, and the production processes with strongly toxic intermediates.

Modification of PFSA membranes are made for operation at high temperature and low humidification levels, improving water management, and reducing fuel crossover. Many efforts have been made to modify PFSA membranes for high temperature operation. The approaches include replacement of water with low volatile and/or non-aqueous media such as phosphoric acid, acetic acid, ionic liquids and heterocycles; the use of thinner membranes and impregnation with hygroscopic oxide nano-particles such as SiO_2, and impregnation with solid proton conductors like heteropolyacids and zirconium phosphate to reduce humidification level; plasma etching and palladium sputtering to lower the fuel crossover. The modified PFSA membranes have been able to operate up to 120°C under atmospheric pressure and up to 150°C under pressures of 3-5 atm [20].

A large variety of aromatic polymers are considered as alternative PEM's because of their low cost, chemical and thermal stability. They are modified with bulky groups in the backbone or aromatic hydrocarbons are directly incorporated into the backbone of a hydrocarbon polymer to make them proton conductive. The examples are liquid crystal aromatic polyesters, PBI's, polyimides (PI), polyetherimides (PEI), polyphenylene sulphides (PPS), polysulphones (PS), polyethersulphones (PES), polyetherketones (PEK), polyetheretherketones (PEEK), polyphenyquinoxalines (PPQ), etc. [15]. These polymers are also used as the host matrix for inorganic/organic composite membranes. The solid inorganic proton conductors include zirconium phosphates and heteropolyacids. Unlike PFSA membranes, the aromatic polymer membranes have less hydrophobic backbones, and less acidic and polar functional groups which result in a reduction in the dependence of conductivity on humidity. Their weak point is that they are not very good proton conductors even at high humidity levels.

Acid-base polymer complexes are produced by doping the polymer networks containing basic (acidic) sites with inorganic acids (bases). The polymer membranes of this type include PBI, polyethylene oxides (PEO), polyvinyl acetate (PVA), polyacrylamide (PAAM), PEI, etc. with the inorganic acid such as H_3PO_4 which is of interest due to its thermal stability and high proton conductivity at high temperatures even in anhydrous form. High acid contents results in high

conductivity but decrease mechanical stability, especially at high temperatures. To have sufficient mechanical strength, polymers are crosslinked, inorganic fillers are used, or polymers having high glass transition temperature (T_g) are chosen.

2.2 General Information about Polybenzimidazole Polymers

PBI polymers are a class of linear heterocyclic polymers containing benzimidazole group in the polymer backbone (Figure 3). They are included in thermoplastics because of their linear chains. There are two types of PBI's: aliphatic PBI's which were first developed by Brinker et al in 1959 [21], and fully aromatic PBI's which were first synthesized by Vogel et al in 1961 [22]. Especially, the fully aromatic ones exhibit excellent thermal stability (T_g > 400°C), high toughness and stiffness, and are resistant to chemicals, acid and basic hydrolysis, and high temperature because of their intermolecular hydrogen bonding, linearity, absence of crosslinking to limit stress-release processes, and highly stable phenyl groups [23], [24]. There are four different structures of PBI's as indicated in Figure 4. The functional groups (R, R' and X) in Figure 4 are listed with their physical and thermal properties by Salamone [24].

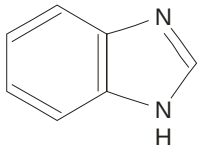

Figure 3. The benzimidazole group

Among the PBI polymers, poly [2,2'-(m-phenylene)-5,5'-bibenzimidazole] (mPBI) is the only commercialized one by Hoechst Celanese Corporation under the trade name of celazole. Extensive study was carried out on this polymer due to its toughness, non-flammability, processability, thermal and chemical stability [24]. It is a fully aromatic PBI the molecular structure of which is shown in Figure 5. It is

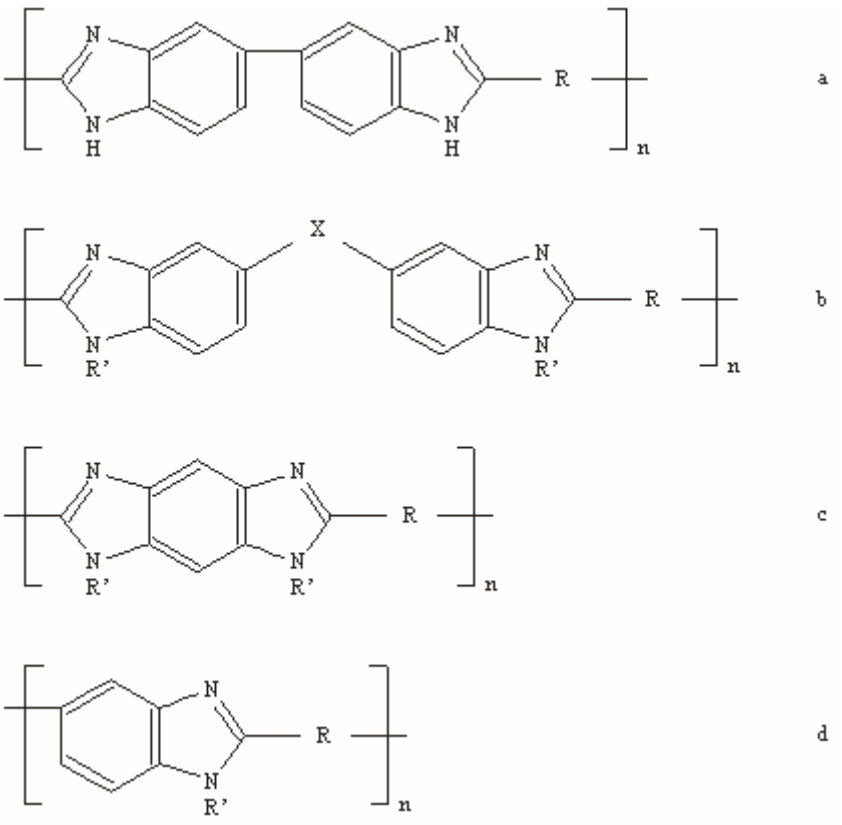

Figure 4. The molecular structures of PBI's

composed of a flexible main chain with the catenation angles of 150°C [25] and so it shows amorphous properties. The presence of three phenyl groups in the repeating unit gives the polymer superior properties. T_g of mPBI is around 430°C, and it has no melting point. Thermogravimetric analysis (TGA) in air showed that it started to decompose at 450-500°C [26]. It is a basic polymer with pKa = 5.5 [23].

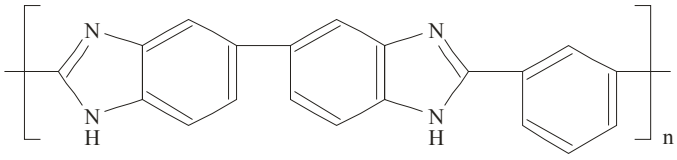

Figure 5. The molecular shape of mPBI

There are a wide spread of application areas for mPBI due to its excellent properties. The high chemical and environmental resistance and mechanical properties lead to the choice of mPBI as reverse osmosis membranes. It is used for sorption of aqueous SO_2 and separation of CO as well as acids because of its high affinity to acids. It is used in space cloths of astronauts, and durable parts of spaceship such as wings. It is non-flammable and non-smoking; when stabilized with sulfuric acid or phosphoric acid, its dimensional stability at high temperatures is improved [24], and then it can be used in protective clothing for firemen. Because of the chemical stability, its application as catalyst support is possible (i.e. Pd/PBI). Due to the high insulation efficiency which prevents electrical current leakage, good heat and moisture resistance make mPBI ideal for semiconductors and electrical circuits. Low dielectric constant and low tangent loss mean low radar observability, and with these properties, mPBI is considered for military applications. It is developed as insulating foam and adhesive (Since it has a completely cyclic structure, it provides foam having high char and ablative characteristics.). When modified with acid doping or implanting, it works as conductive material (i.e. the electrolyte of a PEMFC).

2.3 Synthesis of m-Polybenzimidazole

There are mainly two methods developed for mPBI synthesis: melt/solid polycondensation [22] and solution polymerization [26]. A one stage melt polycondensation method was also proposed in literature [27]. Effect of different catalyst materials was observed in some studies on mPBI synthesis.

The commercial mPBI is synthesized using a melt/solid polycondensation method which is first developed by Vogel et al [22]. The reaction monomers for this method are diaminobenzidine (DAB) as an aromatic tetraamine and diphenyl isophthalate as a dicarboxylic acid derivative. These reactants are put into a reactor, then the inside of reactor is deoxygenated by purging with nitrogen, and the whole reaction is performed under nitrogen atmosphere. A stirrer or agitator is used for mixing the reactants during the reaction. The reaction mixture is heated to melt at

220°C, and after melting, phenol evolution becomes noticeable. Continued heating results in increasing viscosity and is ended when it solidifies. The stirring is stopped and vacuum is applied so that the yellow solid prepolymer foams and most of the liberated phenol and water are removed. Then, the material is cooled to room temperature, pulverized and put into the polymerization tube. It is slowly reheated to 350-400°C under vacuum. The high molecular weight polymer is obtained at this solid state stage of the polymerization. The reaction is given in Equation (2.13a).

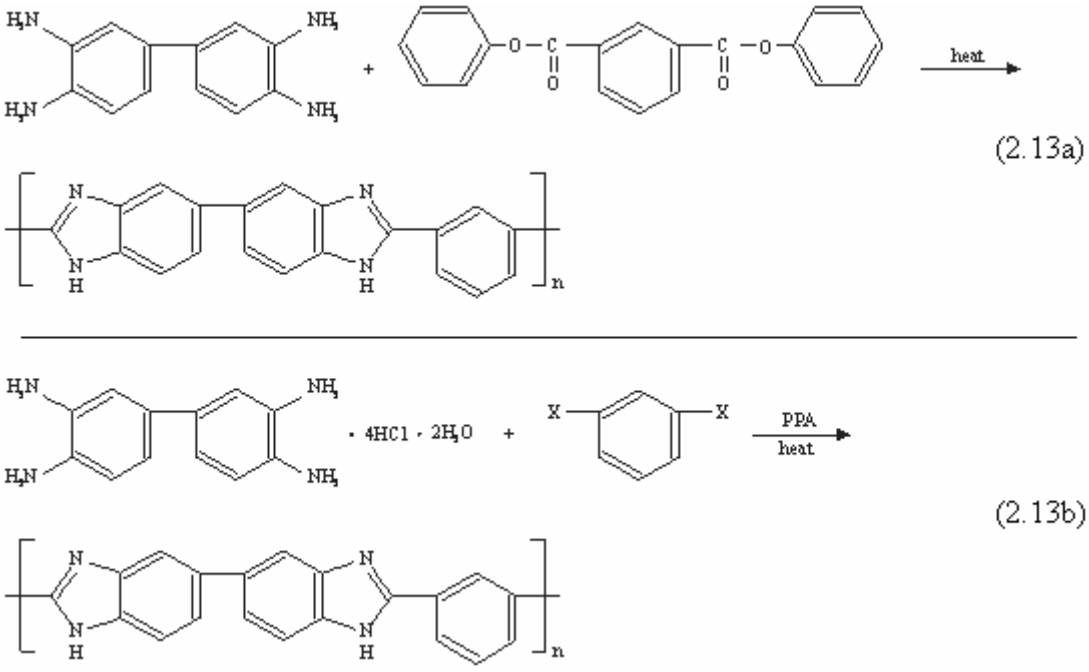

(2.13a)

(2.13b)

For solution polymerization method first found by Iwakura et al [26], [28], diaminobenzidine tetrahydrochloride (DAB.4HCl.2H_2O) is used as tetraamine which is less sensitive to oxidation. An aromatic dicarboxylic acid or its derivative is used as a source of phenylene group in mPBI repeat unit. Polyphosphoric acid (PPA) is used as both solvent and condensing agent for the reactants. The general procedure of this method is as follows: DAB.4HCl.2H_2O and PPA are put into a reactor and DAB is dissolved in PPA at 140°C with a stirrer under a thin stream of nitrogen. The HCl and H_2O molecules are eliminated from DAB as gas bubbles. The aromatic dicarboxylic acid component is added into the reaction solution and the reaction is continued at 170-200°C. At the end of 17 hrs, the polymerization is

ended and the polymer is isolated as a yellowish to brown resinous mass by pouring into DI water. Then, it is dipped into alkaline water, washed thoroughly with DI water and methanol, and finally it is dried. The reaction is shown in Equation (2.13b).

2.4 Phosphoric Acid Doped Polybenzimidazole Membranes

H_3PO_4 doped PBI membrane (PBI/H_3PO_4) is the most successful acid-base polymer complex developed for high temperature operation of PEMFC's. Because PBI contains imidazole rings, it can be doped with acids which make the polymer proton conductive. It has been first proposed by Wainright et al in 1995 [11], and extensive studies have been performed on this type of membrane at Case Western Reserve University, Cleveland, USA. There are numerous studies on conductivity, mechanical strength, gas permeability (P), fuel cell tests etc. of PBI membrane. These studies have shown that this membrane can be operated in PEMFC's up to 200°C with no humidification requirement [11], [20], [29]-[33].

The most widely used PBI in the studies is mPBI due to its superior properties as discussed in Section 2.2. Membranes from this polymer can be obtained by several solution casting methods such as casting from N,N-dimethylacetamide (DMAc) solution [11], NaOH/ethanol solution [34] or TFA/H_3PO_4 solution [35], as well as direct casting from polymerization solution named as sol-gel process [30]. After casting from DMAc or NaOH/ethanol solution, the membranes should be doped with H_3PO_4 by immersing them in a H_3PO_4 solution at room temperature.

The most common method among them is DMAc casting. High molecular weight mPBI's are difficult or incompletely soluble in DMAc, and addition of a minor amount of LiCl in mPBI/DMAc (1-5wt %) is essential for breaking up the aggregates and enhancing the solubility of polymer in the solution, since Cl^- anions in DMAc have greater freedom to disrupt inter and intramolecular hydrogen bonds in mPBI [26], [36]. For complete solution, it is proposed that the solvent should be heated to about 240°C in a pressurized vessel [23]. The concentration of the

solution varies between 5wt% and 20wt% (Below 5wt%, the collapse of polymer chains of mPBI is not sufficient to form compact and complex helical structures for membrane formation, which causes subsequent contraction and expansion in the membrane; above 20wt% [36], it becomes impossible to obtain a homogenous solution).

The membranes prepared from DMAc solution is doped with H_3PO_4 at different levels by immersing into the acid solutions with different concentrations. The immersion time is also important for weight gain due to acid doping and water uptake. There are useful experimental data about the water uptake and acid doping levels of mPBI membranes according to acid concentration and immersion time [20], [32], [37], and these are given in Figure 25-Figure 28 in Appendix B. In Figure 26, it is shown that about 50 hrs of immersion time at room temperature is necessary for membrane to reach its equilibrium doping level in the acid solution. mPBI/H_3PO_4 membranes can involve both dissociated and un-dissociated acid. Of the doping acid, 2 molecules H_3PO_4 are bonded to each mPBI repeat unit. Samms et al. [38] showed by using solid-state nuclear magnetic resonance (NMR) characterization that H_3PO_4 in the PBI membrane is relatively immobile as compared to free H_3PO_4. In a study [37], acid concentration in polymer was found to be much higher than that of acid solution. These results reveal that there is a strong interaction between mPBI and H_3PO_4. Indeed, it comes from the intermolecular hydrogen bonding between H_3PO_4 molecules and N atoms of the imidazole rings instead of protonation of N atom by H_3PO_4 [39].

The conductivity of mPBI/H_3PO_4 membranes depends on acid doping level and temperature. Although it does not restrictively depend on humidity as that of Nafion® because of its almost zero water drag coefficient and that there is an acid medium other than water which acts as both proton acceptor and donor in the complex, increased water vapor activity provides a higher water content in the electrolyte which lowers the viscosity within the membrane, leading to higher mobility and conductivity [11]; water molecules have also a bridging effect in conduction mechanism. The mPBI/H_3PO_4 membranes can have only 2 molecules H_3PO_4/ mPBI repeat unit as bonded acid. However, this acid doping level is not

sufficient, so free acids in the membrane matrix are needed to improve conductivity. The values of conductivity are varying in literature. He et al. [29] found the conductivity as $4.5x10^{-2}$ S/cm for the membrane with 6.6 mole H_3PO_4 doping level, at 110°C and 50% relative humidity (RH), and it increased to 0.10 S/cm for the same membrane at 200°C, 5% RH (same vapor pressure). Lobato et al. [31] obtained $3x10^{-2}$ S/cm of conductivity for 6.2 mole H_3PO_4 doping level at 190°C, in air saturated at 60°C (~1% RH), and Wainright et al. [11] obtained the same value for 5 mole H_3PO_4 doping level at 150°C, 20% RH. Much higher conductivity values (i.e. >0.1 S/cm) were obtained for much higher acid doping levels: Qingfeng et al. [32] found 0.13 S/cm of conductivity for 16 mole H_3PO_4 doping level at 150°C, which was equilibrated with the medium having 80-85% RH at 25°C. Exceptional conductivity values such as 0.26 S/cm for the membrane cast directly from the polymerization solution and having 32 mole of acid doping at 200°C and no humidity were also reported [30].

The proton transfer through mPBI/H_3PO_4 membranes is generally supposed to occur according to the Grotthuss (hopping) mechanism. The evidences are given as follows: the conductivity data mostly fit to the equation of Arrhenius' Law (Equation (2.14)) suggesting a hopping like conduction mechanism; the presence of HPO_4^{-2} and $H_2PO_4^{-}$ anions based on FTIR analysis [39] shows that proton transfer occurs via small charge carriers hopping between phosphorus and imidazole groups; the electro-osmotic drag coefficient is almost zero [40] implying no water and phosphorus dragging or diffusion through the membrane; the conductivity increases as acid content increases by which the distance between clusters of acid sites decreases and the anion moieties support the proton hopping between imidazole sites. Ma et al. [41] gave a chemical structure for proton transfer through the membrane via hopping mechanism (Figure 29 in Appendix C).

$$\sigma = A*\exp(E_a/RT) \qquad (2.14)$$

where A: pre-exponential factor

E_a: activation energy for proton transfer

The conductivity can be increased by increasing acid doping level. However, the mechanical strength of mPBI/H_3PO_4 membranes restricts the doping level,

because as acid content increases after 2 moles of doping level, the membranes become more rubbery and softer, and the mechanical strength significantly decreases. The tensile strength of pristine mPBI is roughly 120 MPa [23] at room temperature; when the mPBI membrane is doped with acid, it could drop to a value as low as 5 MPa at room temperature and 1 MPa at 150°C [20]. Therefore, a compromise between conductivity and mechanical strength should be made to find the optimum acid doping level. In literature, it is usually suggested as 5 mole of acid doping, but it can be increased to higher values by preparing membranes from the mPBI polymers having higher molecular weight and so higher mechanical strength. He et al. [29] showed that increasing molecular weight for mPBI/H_3PO_4 membranes increased the mechanical strength.

The advantages of mPBI/H_3PO_4 membranes are summarized below,

- Good proton conductivity at elevated temperatures (>0.1 S/cm at high acid doping levels)
- FC operation up to 200°C [20]
- Low gas and methanol permeability [42]

  P_{H_2} (150°C) = 6.03×10^{-14} mol.m.m^{-2}.s.Pa

  P_{O_2} (150°C) = 3.35×10^{-15} mol.m.m^{-2}.s.Pa

  $P_{methanol}$ (150°C) = 9.04×10^{-14} mol.m.m^{-2}.s.Pa
- Almost zero electro-osmotic drag coefficient [32] (it means that proton transfer does not include water transport, so a low level of gas hydration can be used without drying out of the membrane, and reactant crossover is reduced.)
- Excellent oxidative and thermal stability up to 200°C [23]

The following aspects are under development for mPBI/H_3PO_4 membranes,

- Determination of long-term stability of the fuel cell characteristics
- Utilization of this approach to develop new low-cost polymer electrolyte membranes

CHAPTER 3

EXPERIMENTAL

3.1 Materials

DAB.4HCl.2H_2O (assay: ≥98%, Sigma-Aldrich) and isophthalic acid (IPA) (assay: 99%, Sigma-Aldrich) as the monomers for the polymer synthesis, and 115% PPA (reagent grade, Sigma-Aldrich) as the condensing agent and solvent for polymerization reaction were purchased. Sodium bicarbonate and methanol (both reagent grades, Merck) as the washing chemicals used for polymer isolation from the reaction solution, and anhydrous $CaCl_2$ (technical grade, Merck) for the drying tube were purchased. 85% o-phosphoric acid (extra pure, Merck) used for acid doping and DMAc (Merck) used for solution casting were bought. 95-98% H_2SO_4 solution (Sigma-Aldrich) used for measurement of polymer viscosity was taken. 540 grade filter papers (Whatman) used for filtering the polymer from reaction solution were purchased. Nitrogen and dry air (BOS) used in the experiments were bought.

3.2 Polymer Synthesis

The mPBI polymer was synthesized by the PPA solution polymerization method. The reaction setup used for polymer synthesis is shown in Figure 6. The monomers were DAB.4HCl.2H_2O and IPA, and the condensing agent and solvent for the polymerization reaction was 115% PPA. The procedure for the synthesis of mPBI was as follows: A specific amount of PPA was put into a three-necked flask equipped with a stirrer, nitrogen inlet and $CaCl_2$ drying tube, and heated to 140°C. The DAB.4HCl.2H_2O which was 1/26.5 of PPA in weight was added gradually and dissolved at 140°C under a thin stream of nitrogen gas and stirring. During dissolving, bubbles were formed on the surface of the reaction solution due to the

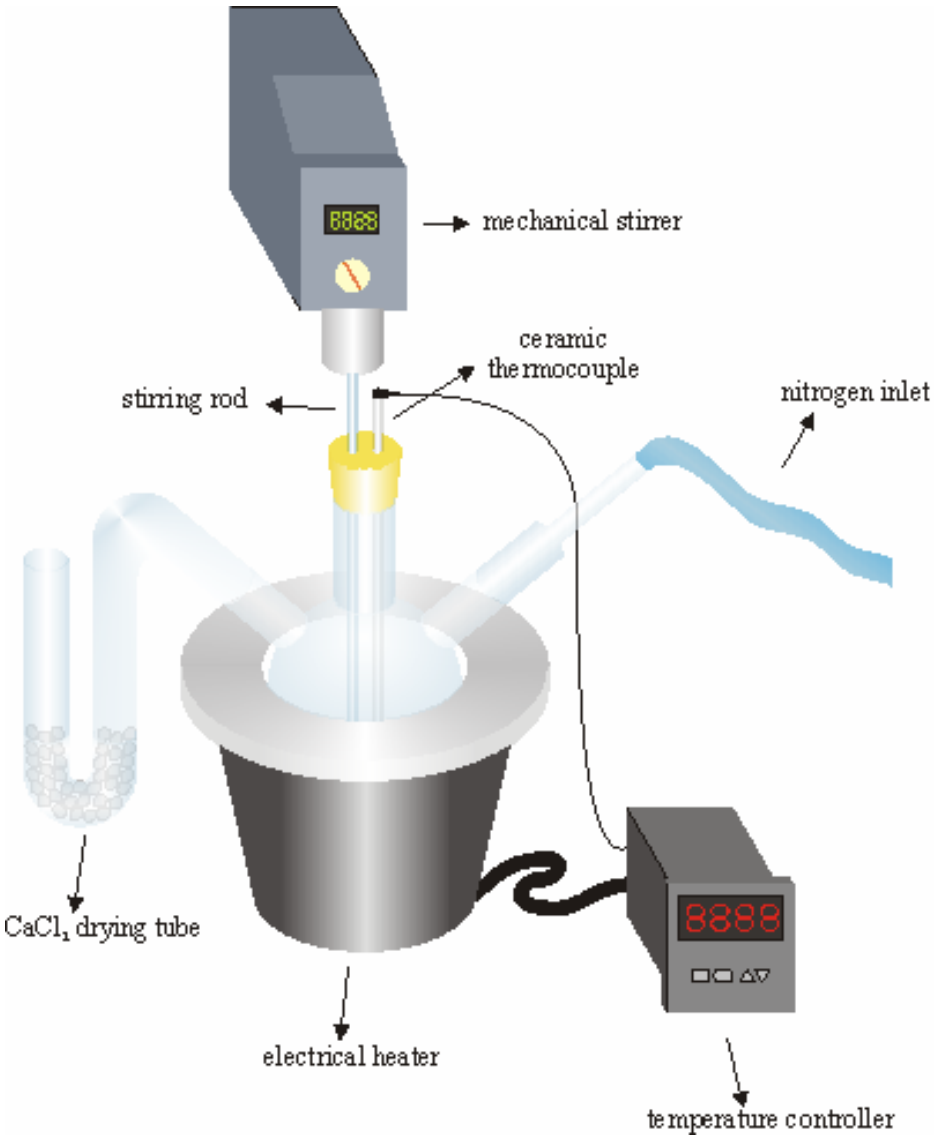

Figure 6. An illustration of the reaction setup for polymer synthe**sis**

elimination of HCl gas from diaminobenzidine molecules. After all bubbles disappeared, an equimolar amount of IPA with the DAB was added into the solution, the stirring rate was decreased, and the temperature was raised to 170°C. The heating was continued at this temperature for 4.5 hrs. Then, the temperature was increased to 200°C, and the reaction was continued between 12 and 24 hrs. The reaction mixture became viscous as the reaction proceeded. The overall reaction of polymerization is given in Equation (3.1).

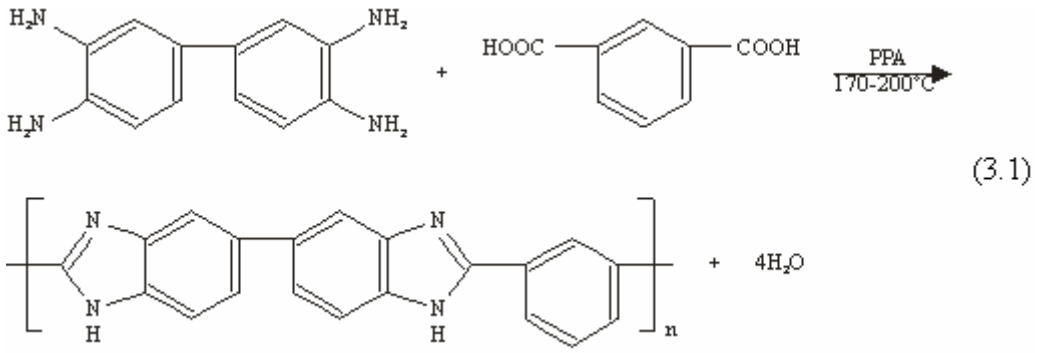

(3.1)

The polymer isolation procedure after the reaction is shown in Figure 7. After the reaction ended, the highly viscous solution was slowly poured into a beaker filled with de-ionized (DI) water at room temperature. Upon precipitation of solid polymer particles at the bottom of the beaker, the liquid was taken out by filtering under vacuum. The precipitate was washed with plenty of boiling DI water, again it was allowed to precipitate, and the liquid was filtered out (pH = 2.5). The precipitate was dipped into a 5wt % $NaHCO_3$ solution and kept overnight under stirring in this solution to neutralize the material. Thereafter, the solution was waited for precipitating and the liquid phase was filtered out (pH = 8.5). The remaining part was washed thoroughly with water and methanol for further isolation of the polymer under vacuum filtering. The resulting pH was measured as 9.0. Then, the solid filtrate was kept in an oven at 150°C overnight. The polymer was obtained as a yellowish to brown resinous mass (Figure 8), which was almost in theoretical amount. Finally, the dried polymer was ground and kept in a dry medium for further use.

3.3 Characterization of the Polymer

3.3.1 Infrared spectroscopy

The infrared (IR) spectrometry of the polymer was analyzed using a spectrometer (Hitachi 270-30). A sample cut from a polymer film with a thickness of 30 μm, prepared by DMAc solution casting, as described in Section 3.4, was used, and the analysis was performed between wavenumbers 4000-400 cm^{-1}.

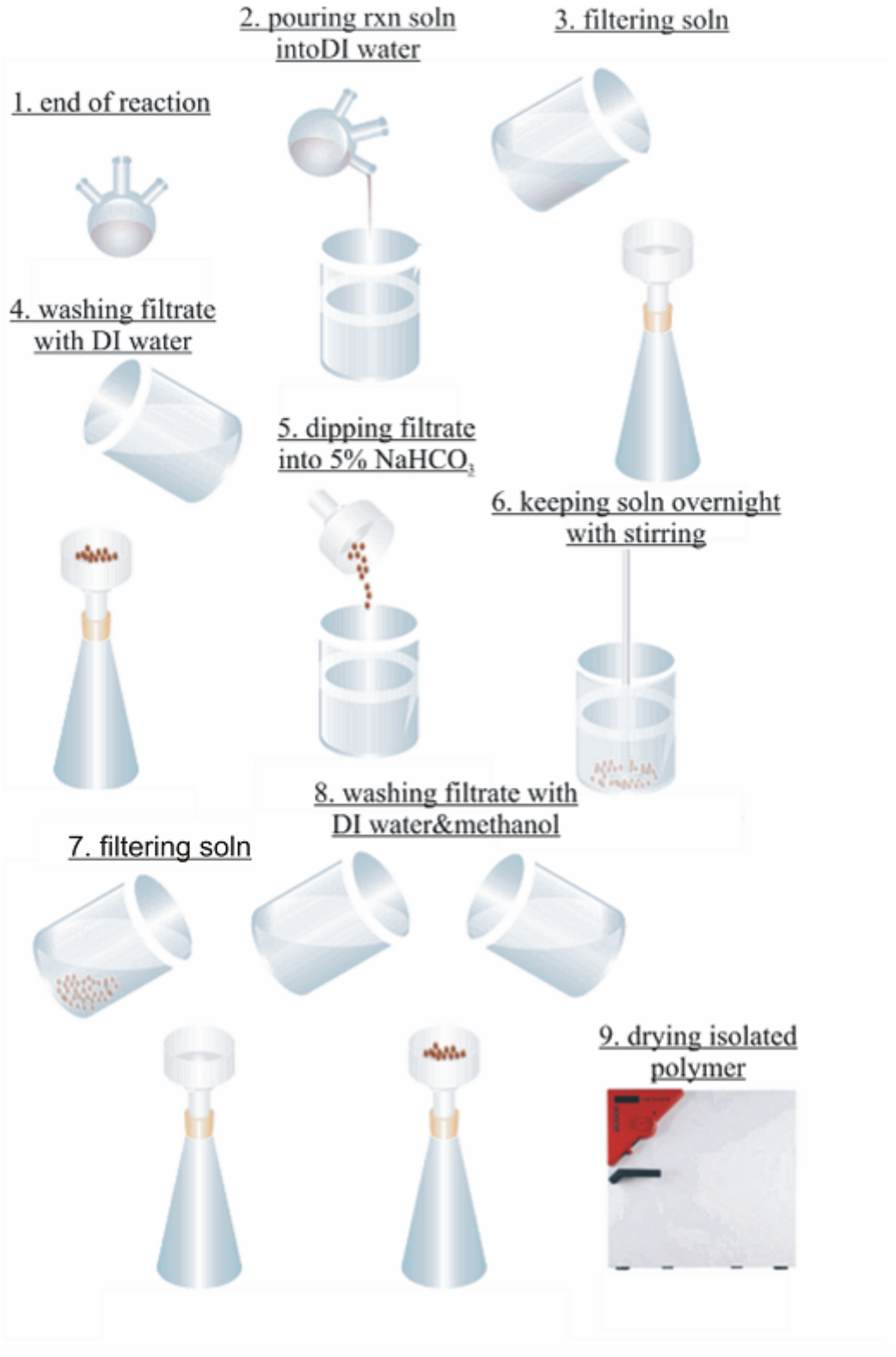

Figure 7. The steps followed for polymer isolation after the polymerization reaction

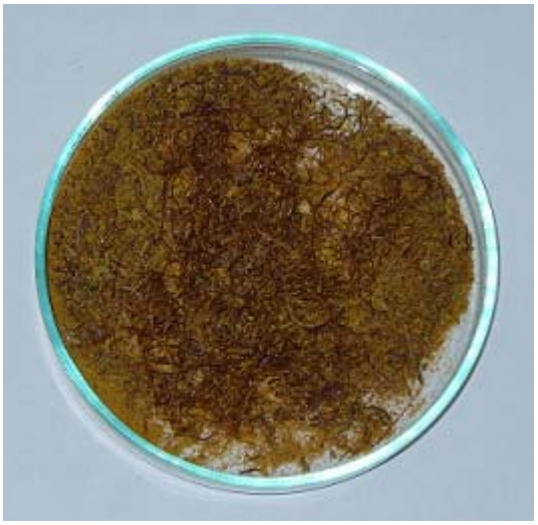

Figure 8. A picture of the powder mPBI polymer synthesized

3.3.2 X-Ray powder diffraction

The analysis of X-Ray spectrometry was performed using a diffractometer (Philips PW1740), employing Cu anticathode radiation. A sample taken from the pulverized polymer was used, and the analysis was done in the 2θ range from 5° to 50° with a scan step of 0.02°/sec.

3.3.3 Nuclear magnetic resonance spectra

The nuclear magnetic resonance (NMR) spectra of pristine mPBI were determined by the analysis of 1H-NMR using a 300 MHz spectrometer (Bruker). The mPBI sample was dissolved in DMSO, and the NMR analysis of this polymer solution was performed at 23°C.

3.3.4 Thermogravimetric analysis

The thermal stability of mPBI polymer was determined using a thermogravimetric analyzer (DuPont 2000). A sample of the polymer powder was heated in dry air at a temperature ramp of 5°C/min up to 600°C, and the weight loss of sample was recorded during this period.

3.3.5 Measurement of the polymer viscosity

The intrinsic viscosities (η_{int}) of the synthesized polymers for determination of molecular weight were measured by using the dilute solution viscosity measurement technique of the Ubbelohde type. For this technique, a home-made Ubbelohde viscometer, which is a glass capillary viscometer in which the polymer solution flows through a capillary under its own head, was used (Figure 9). To measure the flow times at a specific temperature, the viscometer was placed in a water bath and heated by an electrical heater with stirring (Figure 10).

The procedure for viscosity measurement is as follows: First, a polymer solution with a concentration of 1.6g/dl (1dl = 100ml) was prepared by dissolving 0.16 gr of the polymer in sulphuric acid using an ultrasonic bath (SONOREX RH 100H). This solution was used as a stock solution to prepare the polymer solutions

Figure 9. The Ubbelohde viscometer

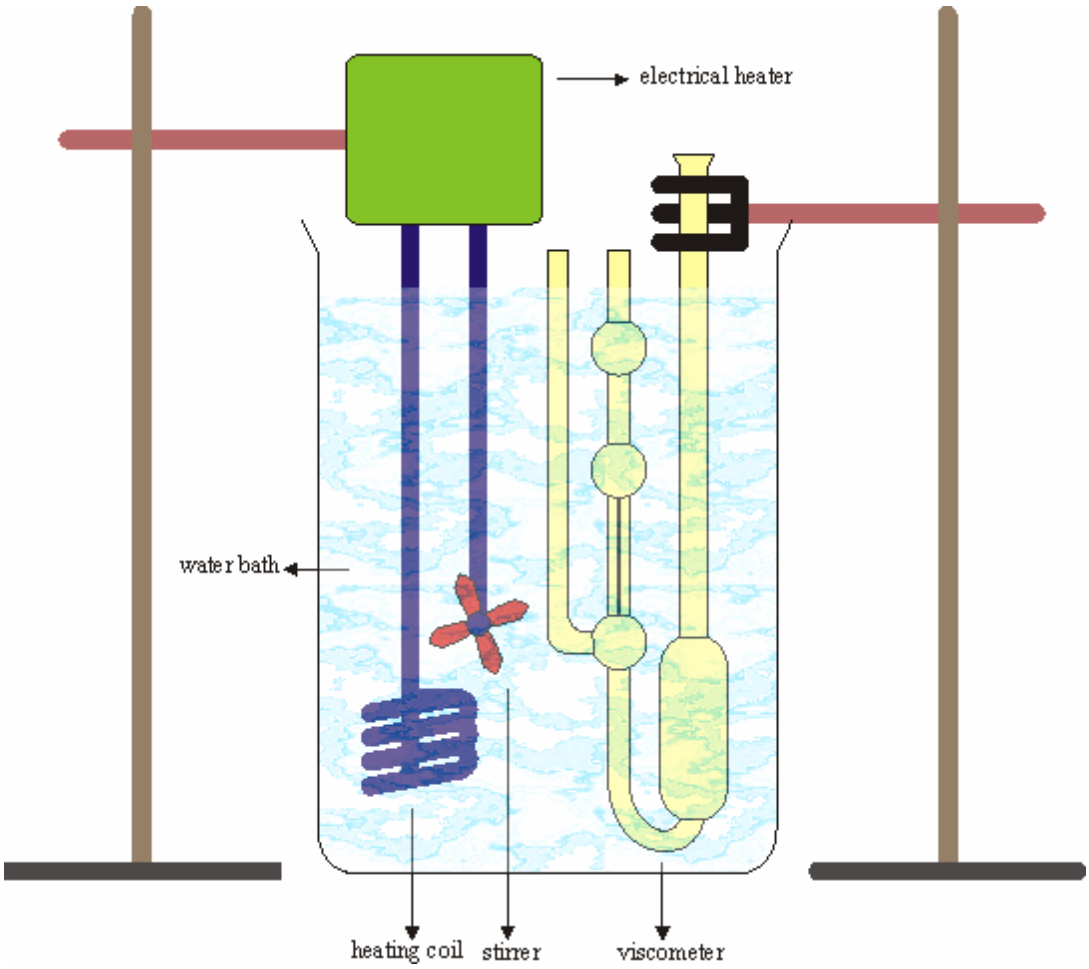

Figure 10. The experimental setup of viscosity measurement

of different concentrations.). Then, the viscometer was put into the water bath, and the efflux time for pure sulfuric acid in the viscometer (t_0), was measured in the viscometer at 30°C. After that, the acid in the viscometer was concentrated by adding from the polymer solution of 1.6 g/dl and the efflux time of the prepared solution (t) was measured at 30°C. This was repeated for totally four different concentrations in the viscometer: 0.4, 0.6, 0.8 and 1.0 g/dl.

3.4 Membrane Preparation

The polymer membranes were prepared by a solution casting method. As solvent, DMAc/LiCl system was used. 5wt% of polymer powder was added to the

solution, and mixed in an ultrasonic bath at 70°C. To prevent the polymer from aggregating, mechanical stirring was also used. The polymer was totally dissolved in DMAc with 2 hrs of stirring, so it was not required to filter the solution. Different portions of the prepared polymer solution according to the desired membrane thicknesses (i.e.30 μm) were cast onto glass plates. Next, the plates were put into a ventilated oven and the solvent was evaporated slowly at 80°C in 15 hrs. After that, the glass plates were immersed into DI water and waited for a couple of minutes. At this step, the polymer film took up water and swelled out of the plate. The films obtained were immersed into boiling DI water and kept for 5 hrs to remove LiCl. Thereafter, the membranes were taken out of the water, put into an oven and kept at 190°C for 3 hrs to remove the solvent traces from the membranes. Finally, their dimensions were measured and they were stored in a dry medium for further use.

3.5 Acid Doping of the Membranes

The membranes cast from DMAc solution were doped with H_3PO_4 by immersing them into H_3PO_4 solutions. Four different acid solutions were prepared to obtain four different acid doping levels: 11, 13, 14 and 14.7 M (the molarity of 85% o-H_3PO_4 solution bought). The membranes were kept in the acid solutions for a month. An example of the prepared membranes is given in Figure 11. During that time, their weights and dimensions increased due to acid doping and water uptake. To find the acid doping level, the membranes were dried in a ventilated oven at 105°C so that the weight gain due to water uptake was eliminated. The weight difference before doping and after drying the membrane was found, which was taken as the weight of acid in the membrane. This was used for calculating the acid doping level in terms of molecules H_3PO_4/mPBI repeat unit using the Equation (3.2).

$$\text{Acid doping} = \frac{\text{weight difference}}{\text{initial weight}} \text{ x } \frac{M_w \text{ of mPBI repeat unit}}{M_w \text{ of } H_3PO_4} \qquad (3.2)$$

where M_w of mPBI repeat unit is 308 g/mol

M_w of H_3PO_4 is 98 g/mol

3.6 Characterization of the Acid Doped Membranes

3.6.1 Thermogravimetric analysis

The weight loss of a 6 mole acid doped mPBI/H_3PO_4 membrane sample was measured by the thermogravimetric analyzer. The analysis was performed in two stages: First, the weight loss of the sample was measured as temperature was increased from 35 to 200°C in dry air at a temperature ramp of 2°C/min. Second, the sample was held at 200°C for 2 hrs and the total weight loss was recorded.

Figure 11. A picture of an acid doped mPBI membrane prepared

3.6.2 Tension tests

The mechanical strength of the membranes was measured with a vertical film stretching device (Lloyd 30K Universal Testing Machine). The initial dimensions of the samples were 15 mm in width (w_m), 60 μm in thickness (t_m) and 30 mm in length (l_m). The experiments were performed with a constant stretching speed of 5 mm/min in ambient air.

3.6.3 Conductivity measurement

Ionic conductivities of the membranes were measured by means of the four-probe impedance method using a G 300 Series Potentiostat with EIS 300 Software (Gamry Instruments). The impedance measurements were performed in a frequency range from 1Hz to 100 kHz. The membrane samples were prepared as rectangular pieces with w_m = 9mm, l_m = 50 mm and t_m = 60 μm, and placed in a Teflon conductivity cell with four Pt electrodes (Figure 12, Figure 13). The distance between the two inner electrodes (D) used for measuring the potential difference through the sample was 25 mm. The current was sent over the two outer electrodes.

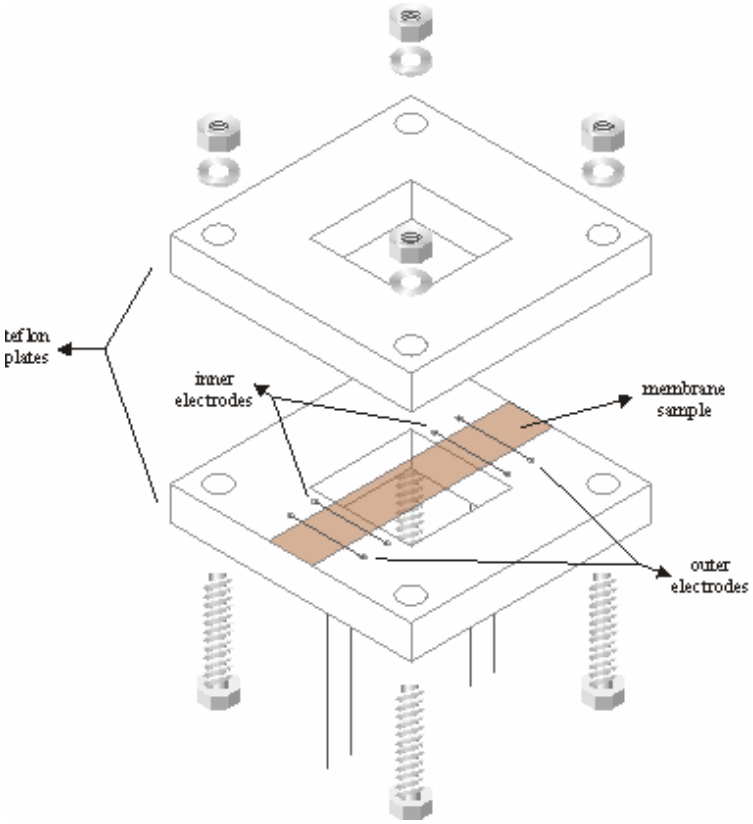

Figure 12. The diagram of conductivity cell

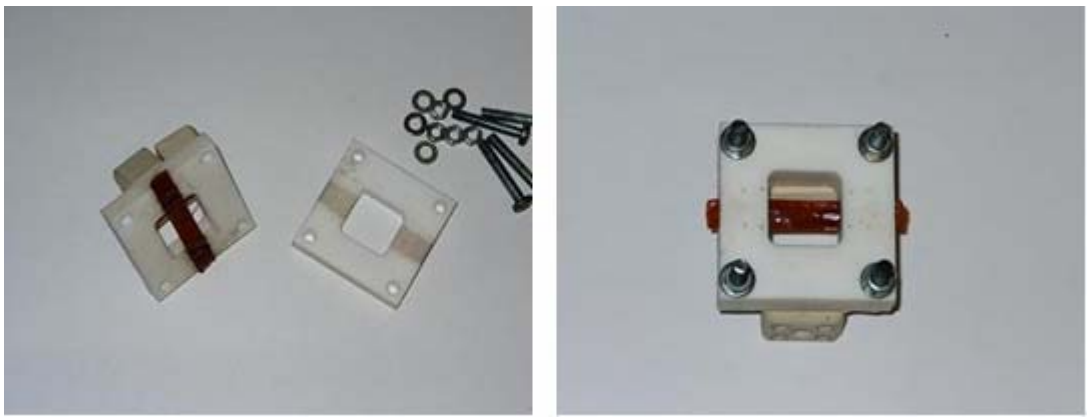

(a) (b)

Figure 13. The open form (a) and the closed form of the conductivity cell used in the conductivity measurements

The conductivities of the membranes at high temperatures and different humidity levels were measured in a humidity chamber designed as shown in Figure 14. It was a stainless steel vessel durable to high temperature, humidity and pressure of several bars. The top of the vessel was designed as a flange, so that it could be easily removed from the main part to mount the conductivity cell into the vessel. To connect the four electrodes of the conductivity cell with those of the potentiostat (reference, working, working sense and counter electrodes), four nickel wires were passed through the flange, and the matching electrodes were connected to the ends of each wire. These nickel wires were insulated from each other and the flange by using a silicon material for high performance gaskets. Heating of the chamber was accomplished by an electrical heating jacket and the temperature inside the vessel was controlled by a temperature controller (GEMO Electronics) with a Pt100 thermocouple. The pressure inside the chamber was read from a KL 1.0 rustproof manometer (Pakkens), which was mounted onto the top of vessel. A vacuum pump, which was used to vacuum the air inside the chamber, was connected to one of the gas outlet branches. To humidify the cell, a measured amount of water was sent into the vessel via pumping it through the water inlet on the flange by a hand pump, after the vessel was vacuumed to zero pressure. For conductivity measurements in dry air, a gas inlet stream used for sending dry air into the system was also placed

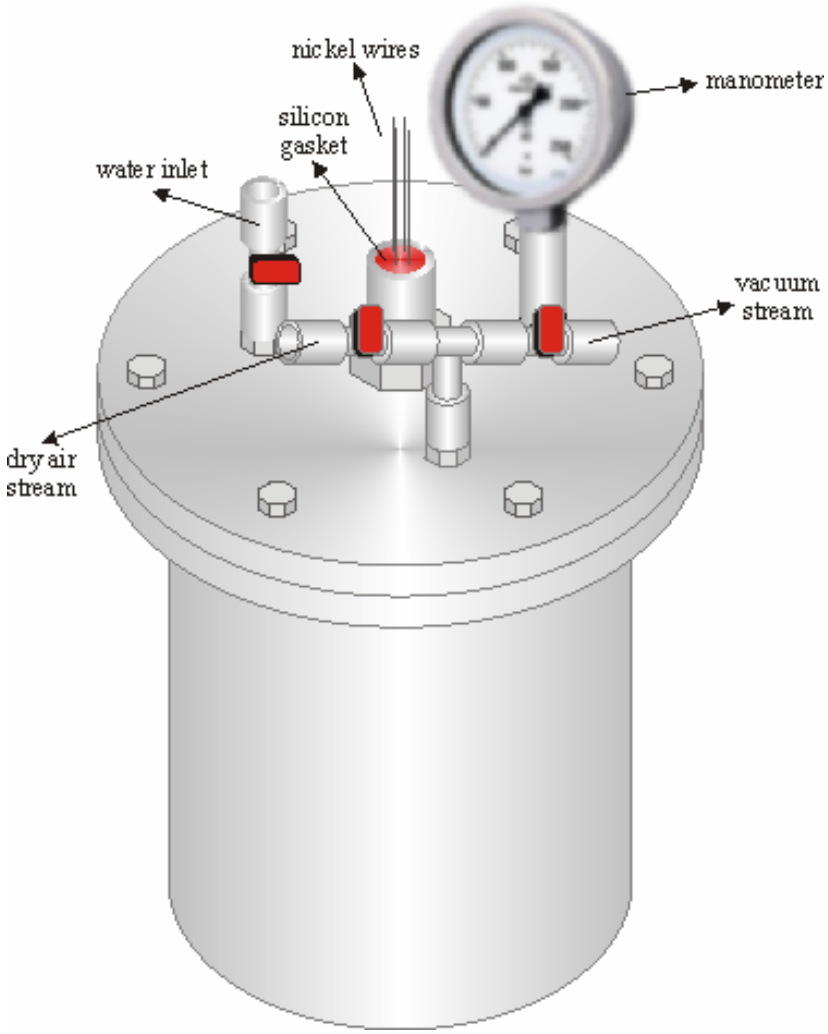

Figure 14. 3D view of the humidity chamber

onto the flange. The complete system used for the conductivity measurements at high temperatures is shown in Figure 15.

The conductivity measurements were performed in the humidity chamber for four different acid doping levels (6, 8, 10 and 11 molecules H_3PO_4/PBI repeat unit) at three different temperatures (110, 130 and 150°C) in both dry air (at atmospheric pressure) and humid medium. The humidity level at each temperature was calculated according to the reading from the manometer. The calculation of humidity levels is shown in Appendix D. The RH was equivalent to 42% at 110°C, 37% at 130°C and 33% at 150°C. The conductivity was also measured for the

membrane having acid doping level of 6 moles in ambient atmosphere at 18°C and 45% RH, to have an idea about the conductivity level of mPBI membranes at low temperatures. The conductivity measurements in humid medium were performed after keeping the membrane sample at each experimental condition for 30 min to let it reach equilibrium with the medium.

To see whether the conductivity measurement system was reliable or not, the conductivity of a known membrane was also measured in the same system. A sample of Nafion 112 membrane was first treated with 1 M sulfuric acid solution to eliminate all ion impurities in the membrane which would affect the conductivity. Then, it was kept overnight in the humidity chamber filled with enough water for 100% RH at 80°C to make sure that the membrane reached equilibrium with the water vapor. Finally, the conductivity was measured at 80°C and 100% RH.

Figure 15. A picture of the complete setup used for the conductivity measurements

The conductivity values were calculated from the impedance data. When the impedance analysis in the specified frequency range was performed, the Bode or Nyquist plot was plotted. From either of these plots, the real part of impedance at which the imaginary part was equal to zero was found. It gave the resistance of membrane (R_m), and this value was used for calculating conductivity from Equation (3.3).

$$\sigma = \frac{D}{w_m \times t_m \times R_m} \qquad (3.3)$$

CHAPTER 4

RESULTS AND DISCUSSION

4.1 Polymer Synthesis, Intrinsic Viscosity and Molecular Weight

The polymer was synthesized using the method of PPA solution polymerization as described in Section 3.2. The main purpose of the synthesis reaction was to obtain a polymer with high molecular weight (i.e. intrinsic viscosity (η_{int}) = 1.3 dl/g (1 dl = 100 ml)). For this purpose, two of the reaction parameters, the reaction time and the stirring rate, were varied to find the best conditions for the synthesis. First, the reaction time at 200°C was optimized by changing it between 12 and 24 hrs. It was observed that the molecular weight of synthesized polymer increased when the reaction time was increased from 12 to 17 hrs, but it was also shown by performing experiments at 20.5 and 24 hrs that the quality of the polymer was not affected by further increase in the reaction time above 17 hrs. After the effect of time was observed, the stirring rate was varied. The important point was that the value of stirring rate had not been published anywhere in the literature. To observe the effect of stirring rate and determine a suitable value, two series of reactions were performed: after the first reaction was performed at a value of stirring rate, the next one was performed at a certain value which was 1/3 of the former one. For example, the preceding reaction, performed to obtain 4.5 gr of mPBI, was stirred with 1000 rpm, while the subsequent one was stirred with 300 rpm which was approximately 1/3 of the former one. At the end of reactions, it was observed that the molecular weight of polymer for the reaction with lower stirring rate was much higher than that with the higher one, and it was a sufficient value for preparing mechanically strong membranes. Thereafter, the synthesis reactions were continued according to the parameters at which polymers with sufficient properties could be obtained. The selected parameters of synthesis reaction are given in Table 2.

Table 2. The results of polymer synthesis

sythesis no.	**1**	**2**	**3**	**4**	**5**	**selected**
T(C) at IPA addition	140	140	140	140	140	-
stirring rate (rpm)	1000	1000	1000	1000	300	300
reaction time at 200C (hrs)	12.0	17.0	20.5	24.0	17.0	17.0
mPBI-synthesized (gr)	4.46	4.55	4.54	4.57	4.60	-
mPBI-theoretical (gr)	4.65	4.65	4.65	4.65	4.65	-
yield%	0.96	0.98	0.98	0.98	0.99	-
η_{int} (dl/g)	0.3	0.9	0.8	0.9	2.1	-
M_w^{av}	11000	43000	37000	43000	126000	

The values of η_{int} for synthesized polymers were determined by dilute solution viscosity measurements as described in Section 3.3.5. The calculation of η_{int} is shown in Appendix E, and the results are given in Table 2. The highest one was calculated as 2.1 dl/gr at 30°C which was actually higher than those of the mPBI polymers used in literature. He et al. [29] used mPBI polymer having η_{int} = 0.6 dl/gr at 30°C. Xiao et al. [30] used polymer with high intrinsic viscosity (1.3-2.0 dl/gr at 30°C) to cast the membranes directly from the polymer reaction solution (In this method, membranes had high acid doping levels such as 32 mole acid per polymer unit, so the mechanical properties should be high for this method.).Lobato et al. [31] synthesized polymers having η_{int} = 1.0 dl/gr at 30°C. It can be easily seen that the polymers used in this study had rather high η_{int} and high mechanical strength, which allowed the prepared membranes to be doped with acid at higher levels.

The average molecular weight (M_w^{av}) of the polymer was found by using the Mark-Houwink equation given in Equation (4.1)

$$\eta_{int} = K\,(M_w^{av})^{\alpha} \qquad (4.1)$$

where K, α : constants, $K = 1.94 \times 10^{-4}$ and $\alpha = 0.791$, respectively [43]

According to the Equation (4.1), the value of M_w^{av} for each synthesized polymer was calculated, and the results are tabulated in Table 2.

4.2 Results of the Characterization of m-Polybenzimidazole

4.2.1 The analysis of infrared spectroscopy

The IR absorption spectra of the synthesized mPBI are shown in Figure 16. The sharp peaks are at 1620, 1528, 1438, 1280 and 796 cm^{-1}. These peaks indicate C=C and C=N bonds, the characteristic of 2-substitution, the characteristic of substituted benzimidazole in plane vibration, the C-N stretch, and the three adjacent hydrogens in six-membered ring (C-H out-of-plane bend), respectively [23]. The description of all peaks including weak and medium ones in the IR spectra shown in Figure 16 is given in Table 8 in Appendix F.

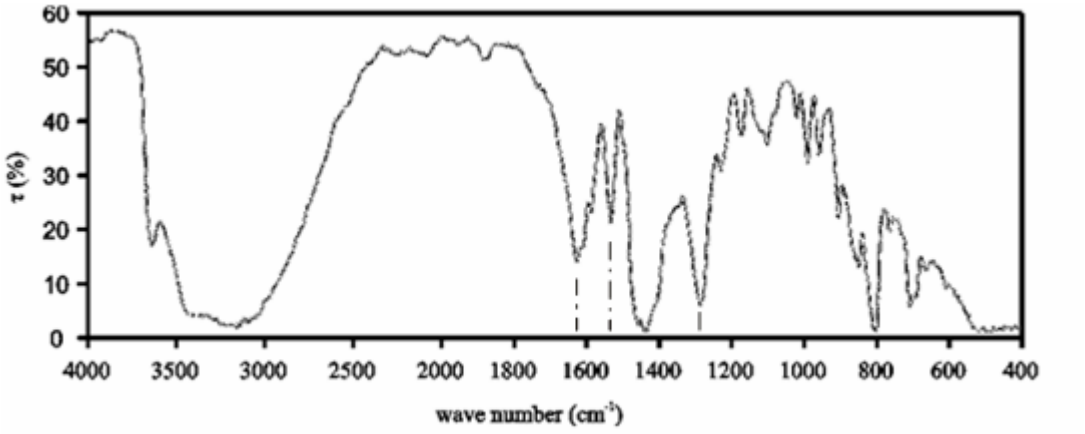

Figure 16. The Infrared spectra of the synthesized mPBI

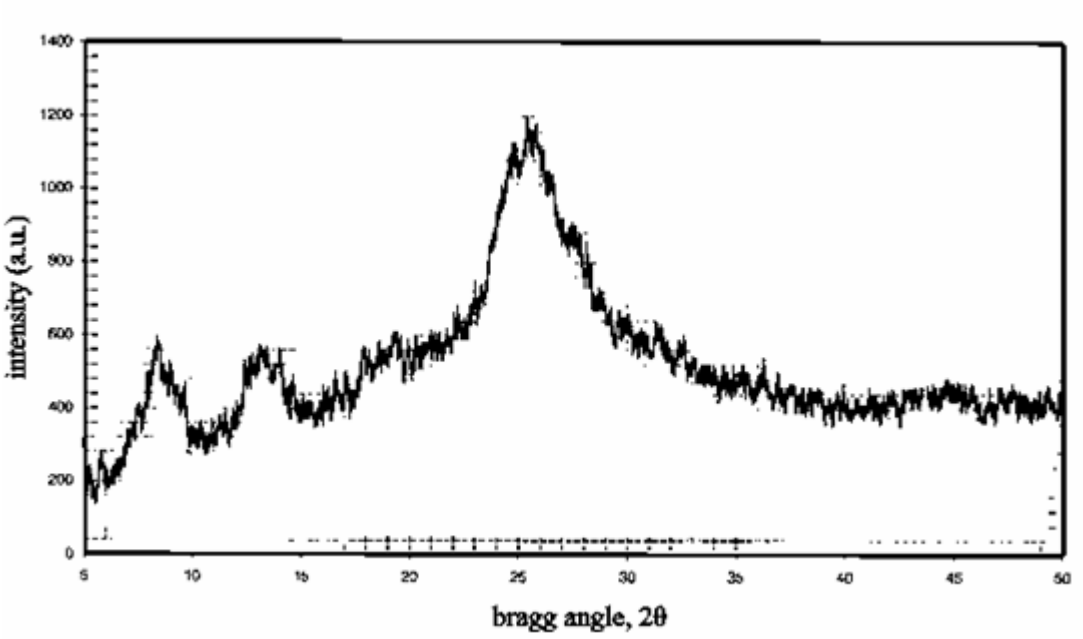

Figure 17. The X-Ray diffraction diagram of the synthesized mPBI

4.2.2 The analysis of X-Ray diffraction

The X-Ray diffraction patterns of the synthesized mPBI are indicated in Figure 17 (An example of XRD pattern of mPBI in literature is given in Figure 31 in Appendix G.). The crystallinity of mPBI was observed by this analysis, and it was shown that the synthesized mPBI was a highly amorphous material with a wide diffraction peak at 2θ = 25°. Carollo et al. [44] referred this peak to the parallel orientation of the benzimidazole rings with respect to the film surface.

4.2.3 Nuclear magnetic resonance spectra

The proton chemical shifts of mPBI were determined by 1H-NMR. The NMR spectra are given in Figure 18. The peak at 13.3 ppm indicates the proton of imidazole ring, and the peaks between 7.65 and 9.15 ppm are due to the proton signal of phenyl groups [45]. In a previous study by Ainla et al. [46], the NMR peaks were obtained at 13.28, 9.16, 8.34, 7.84, 7.80, 7.69, 7.63 ppm, with which those obtained in this study are consistent.

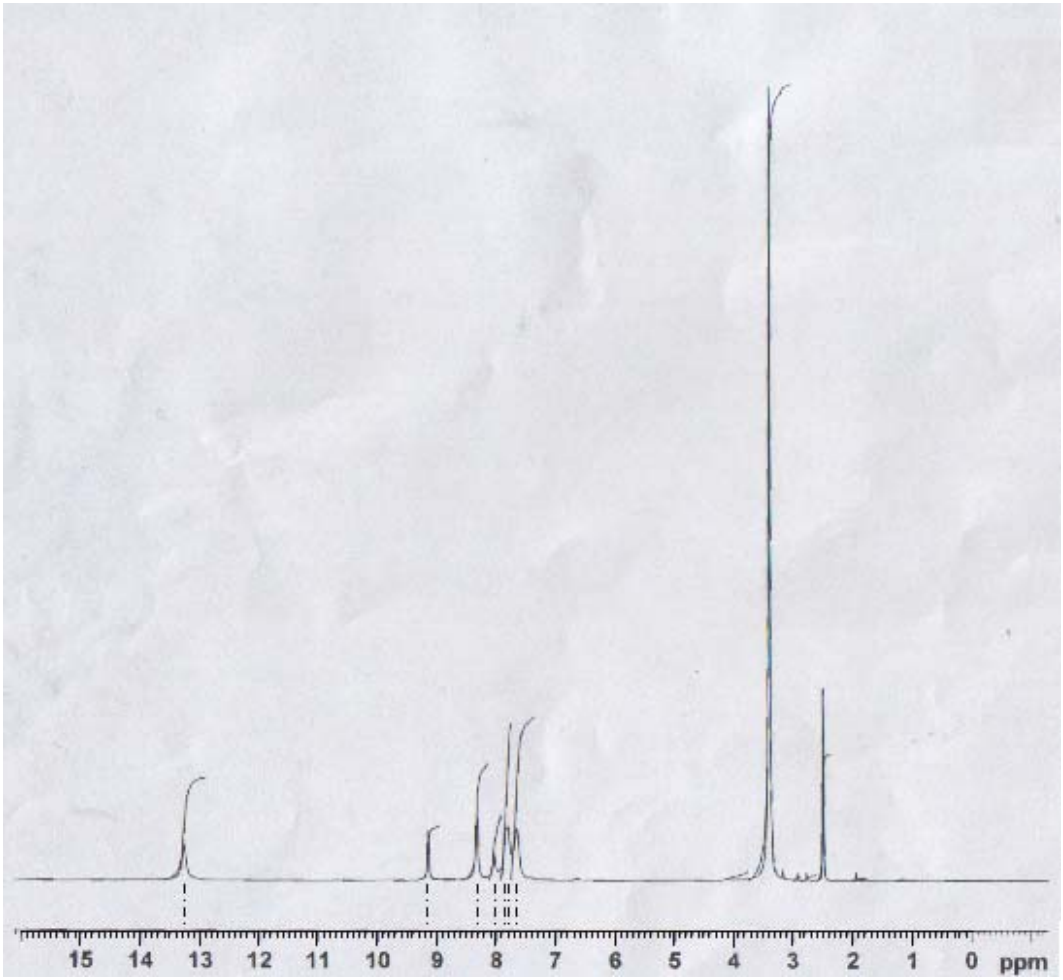

Figure 18. H-NMR spectra of the synthesized polymer

4.2.4 Thermogravimetric analysis

The thermal stability of the synthesized mPBI was determined by TGA. The analysis is shown as weight loss % vs. temperature including the derivative of weight loss in Figure 19. After the weight loss due to removal of absorbed water in the mPBI, no significant change in the weight of sample polymer was observed up to 450°C. After 450°C, the polymer decomposition occurred leaving a black residue.

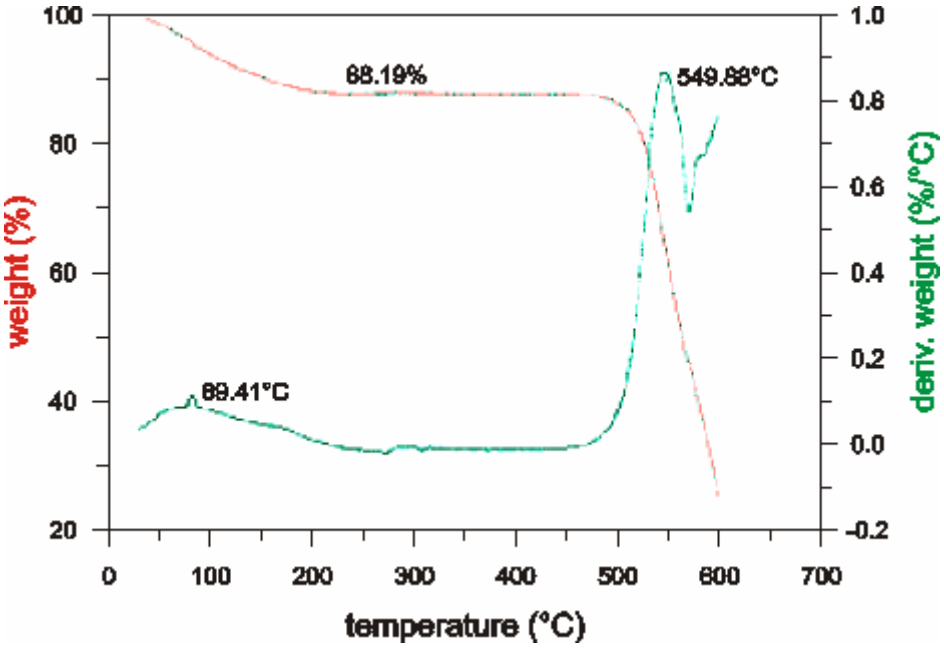

Figure 19. TGA of the synthesized polymer

4.3 The Procedure of Membrane Preparation

The pristine mPBI membranes were prepared via a solving procedure described in Section 3.4. The polymer was dissolved via a procedure different from those in the literature. The polymer is generally dissolved in DMAc/LiCl solvent system for 3 hrs at 250°C in a bomb reactor. The solution is required to be free from oxygen by bubbling an inert gas for 2-3 hrs before closing the reactor, to prevent gel formation and cross-linking at high temperatures. In the procedure used in this study, there was no need to use a pressure compensated reactor excluded from oxygen; instead, the polymer was dissolved in DMAc/LiCl in a glass bottle by mixing the solution for max 2 hrs at 70°C with an ultrasonic bath. Because the temperature level was low, there was no need to exclude oxygen from the solution. The polymer was dissolved completely at all times which eliminated the step of solution filtration.

In a study of the solubility behavior of mPBI in DMAc, it was found that rate of solution was temperature dependent and the complete dissolution occurred if the solvent was heated to about 240°C [23], which seems to be contradictory with

the procedure used in the present study, at first glance. However, ultrasonic stirrers emit ultrasonic sound waves; during the propagation of ultrasonic waves in liquid, secondary effects such as cavitation, acoustic flow and pressure were raised. These effects cause intensive turbulent flows throughout the liquid which considerably diminish the thickness of diffusion layer. The acoustic vibrations also affect the physical and chemical properties of the solution by accelerating the redox reactions and decreasing the gas content in the liquid. Therefore, using an ultrasonic stirrer for solving mPBI in DMAc/LiCl accelerated the dissolution rate and decreased the required temperature level.

4.4 Acid Doping Levels of the Membranes

Different acid doping levels were obtained by immersing the membranes in different acid solutions. By using Equation 3.2, the doping levels were calculated as 6, 8, 10 and 11 mole H_3PO_4 for the membranes dipped into the acid solutions having concentrations of 11, 13, 14 and 14.7 M, respectively. The immersion time was about one month which was actually an excessive level. In literature, 50 hrs of immersion time was found to be enough for an mPBI membrane to reach saturation in a H_3PO_4 solution, as seen in Figure 26 in Appendix B [37]. The reason why it was waited for such a long time was not on a technical basic: a delay occurred in preparing the apparatus of conductivity measurement, and the membranes prepared for the characterization had to be kept in the acid solutions until the apparatus was ready. Indeed, there were no significant differences between the acid doping levels obtained in the present study and previous ones. Only the conductivity levels of 6 and 8 moles were obtained a little bit higher than those in the literature (as seen from Figure 25 in Appendix B, about 5 and 7.5 moles, respectively) which might be the result of water evaporation from the acid solutions during the immersion time.

4.5 Results of the Characterization of Acid Doped Membranes

4.5.1 The thermogravimetric analysis

The TGA diagrams are given in Figure 20 (weight loss vs. temperature) and Figure 21 (weight loss vs. time). The TGA measurement was performed for the membrane doped with 6 mole H_3PO_4. It indicated that there were two significant weight loss ranges with increasing temperature. The first one appeared between 35 and 100°C due to the loss of free water, and the latter one appeared between 120 and 200°C because of the loss of water by acid dehydration. Besides, the weight loss continues slightly when the sample was held at 200°C for 2 hrs which was the result of further acid dehydration.

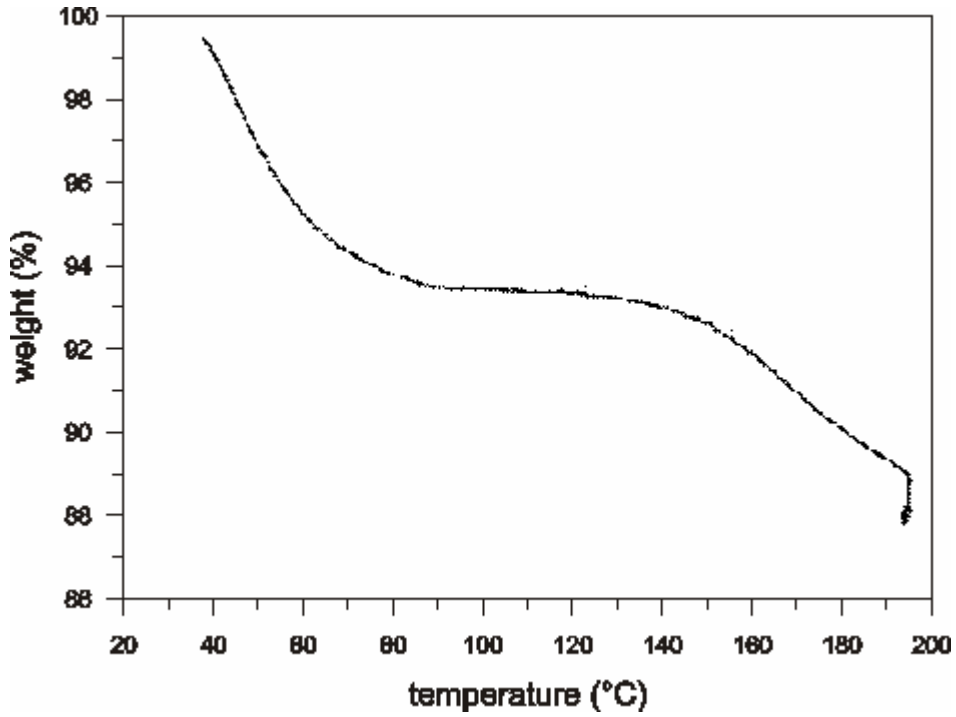

Figure 20. The graph of weight loss vs. temperature of the sample membrane

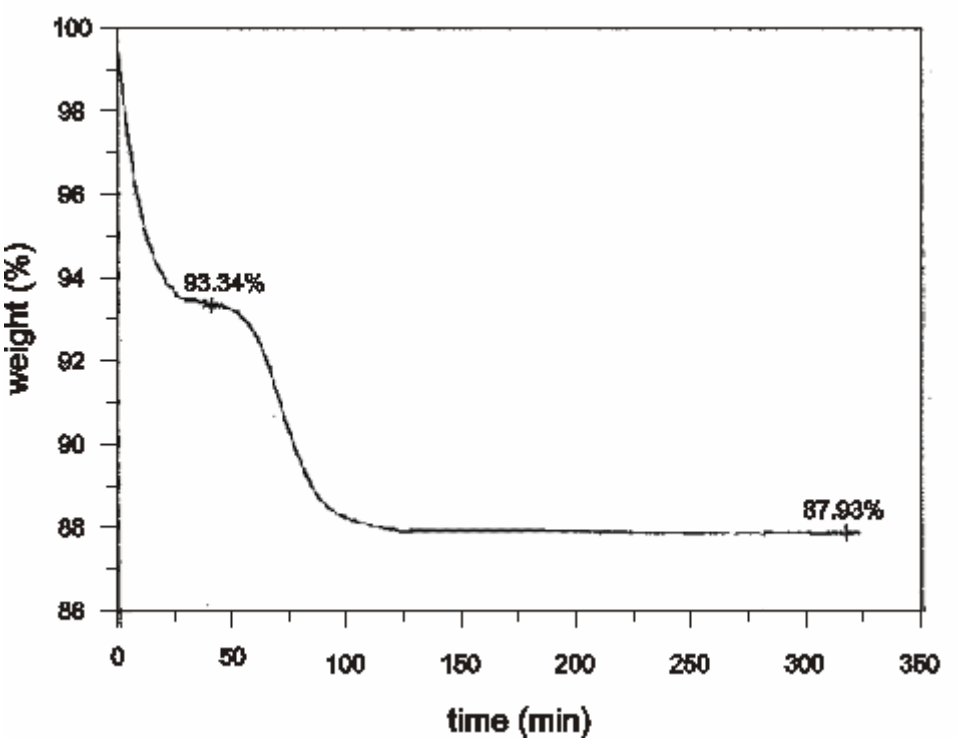

Figure 21. The graph of weight loss vs. time of the sample membrane

The phosphoric acid loses water by dehydration to pyrophosphoric acid (Equation (4.2)), and it further dehydrates to triphosphoric acid (Equation (4.3)).

$$2H_3PO_4 \rightarrow H_4P_2O_7 + H_2O \quad (4.2)$$

$$H_4P_2O_7 + H_3PO_4 \rightarrow H_5P_3O_{10} + H_2O \quad (4.3)$$

The membrane with a doping level of 6 mole acid has 66 wt % of H_3PO_4 and 34 wt % of polymer. Because two of the 6 mole acids are bonded to the two imidazole groups by intermolecular hydrogen bonding, there are 4 moles of free acid/PBI repeat unit which act as concentrated phosphoric acid solution held by the polymer matrix. The concentration of the concentrated solution at 100°C is around 85 % [41]. Therefore, the total amount of water in the matrix is about 7 wt %. The weight loss between 35 and 100°C was 6-7 wt %, which was consistent with the theoretical amount. If the total amount of acid in the matrix dehydrates to pyrophosphoric acid via Equation (4.2), the water produced is 6 wt %. The weight

loss in the second stage (130-200°C) was 5-6wt %, and it can be easily said that it was due to the dehydration of H_3PO_4 molecules via the first reaction.
Dehydration of the acid was shown to be reversible and that the acid regained the water when it was kept at lower temperatures (i.e. 110°C) in humid medium [41]. Therefore, the dehydration is just a reversible process and does not imply degradation of the membrane.

4.5.2 The mechanical tests

The tension tests were performed for the membranes with the highest η_{int} (η_{int} = 2.1 dl/g), at four different acid doping levels. The results of the tension tests for the acid doped membranes are shown in Table 3 and Figure 22. These results showed that the mechanical strength decreased with increasing acid doping level. The highest tensile stress was 23 MPa at the acid doping of 6 moles, while the lowest one was measured as 11 MPa at the acid doping of 11 moles. The elongation was high due to the high doping levels: it was as high as 100% for the doping level of 11 moles.

Table 3. The stress data from the tension tests

acid doping level (mole H_3PO_4/mPBI unit)	**6**	**8**	**10**	**11**
force at break(N)	20.78	14.70	11.18	10.22
w_m (mm)	15	15	15	15
t_m (mm)	0.06	0.06	0.06	0.06
stress(MPa)	23	16	12	11

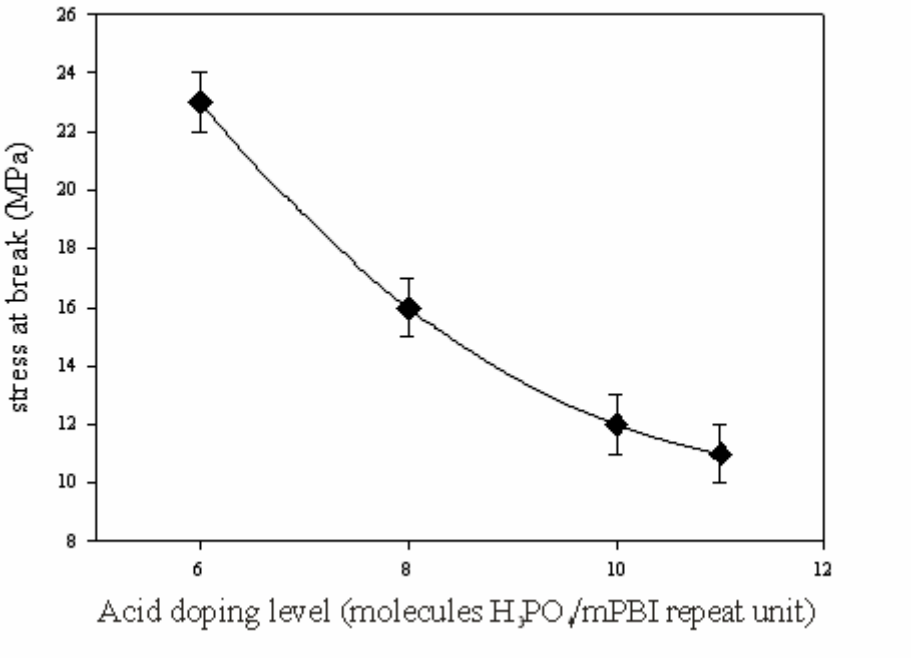

Figure 22. The results of tension tests for the membranes with different acid doping levels having η_{int} = 2.1 dl/g

The mechanical properties of mPBI increases at or below the maximum amount of acid bonded (2 molecules H_3PO_4/mPBI repeat unit). The reason can be explained as follows: For pure polymer, the high mechanical strength is due to hydrogen bonding between –N= and –NH- groups in the polymer structure (120 MPa of tensile stress in average [23]). When H_3PO_4 is introduced all of which is bonded, stronger hydrogen bonds between –N= in the imidazole groups of mPBI and -H- in H_3PO_4 are formed. This further increases the modulus and toughness [11]. However, as the acid doping level is increased above 2 moles of acid, and the mechanical properties significantly decrease. The reason is that when the acid gets into the matrix, volume swelling occurs in the membrane, the distance between the polymer chains increases which cause reduction in the intermolecular forces and so the mechanical strength is decreased. Besides, the membranes become more rubbery and the polymer chains are more flexible to rearrange under load at high acid doping levels, and so the elongation at break increases. These results were

obtained in the mechanical tests of the prepared membranes. The mechanical strength of the membranes was as low as 11 MPa at room temperature when the acid doping level was 11 moles. The membranes were also highly visco-elastic due to the high doping levels, especially for the doping levels of 10 and 11 moles.

4.5.3 The conductivity

The conductivity was measured for four different acid doping levels at three different temperatures in both dry and humid air. The results of conductivity measurement are given in Table 4 and Figure 23. It was indicated that the conductivity increased as the acid doping level and temperature increased. The humidity also had a positive effect on the conductivity, but acceptable conductivity levels were obtained in dry conditions.

The highest conductivity was measured as 0.12 S/cm for the membrane having an acid doping level of 11 moles at 150°C and 33% RH (This value is consistent with those in the literature: Qingfeng et al. [32] found a conductivity value of 0.13 S/cm for a 16 mole acid doped PBI membrane at 150°C.) It was also seen that the conductivities with acceptable levels (>0.01 S/cm) were obtained in dry conditions. A conductivity of 0.054 S/cm was measured for the same membrane at 150°C in dry air. This result is important for FC operation without humidification. For the acid doping level of 6 moles, the conductivity was found as 0.034 S/cm at 110°C and 33% RH. He et al. [29] obtained a conductivity of 0.045 S/cm for the membrane with 6.6 mole acid doping level at 110°C and 50% RH which was comparable with that obtained in this study.

The measurements indicated that the conductivity increased with increasing acid doping level and humidity. The reason is that both phosphoric acid and water are the active components in proton hopping inside the electrolyte (Figure 29 in Appendix C). The effect of temperature was same as those of acid level and humidity. This can be explained by the activation volume (the volume required for the ions and molecules to move through the membrane). It was reported in literature that the activation volume of mPBI/H_3PO_4 was measured as 4-7 cm^3/mole, and it

Table 4. The conductivity values of the membranes (S/cm)

	110°C		130°C		150°C	
acid doping level (mole)	*dry air*	*humid air (42%)*	*dry air*	*humid air (37%)*	*dry air*	*humid air (33%)*
6	$1.91x10^{-2}$	$3.37x10^{-2}$	$2.63x10^{-2}$	$4.81x10^{-2}$	$2.67x10^{-2}$	$6.83x10^{-2}$
8	$2.74x10^{-2}$	$4.82x10^{-2}$	$3.56x10^{-2}$	$6.52x10^{-2}$	$3.65x10^{-2}$	$8.90x10^{-2}$
10	$3.76x10^{-2}$	$6.17x10^{-2}$	$4.58x10^{-2}$	$8.12x10^{-2}$	$4.72x10^{-2}$	$1.10x10^{-1}$
11	$4.37x10^{-2}$	$6.81x10^{-2}$	$5.26x10^{-2}$	$9.08x10^{-2}$	$5.38x10^{-2}$	$1.19x10^{-1}$

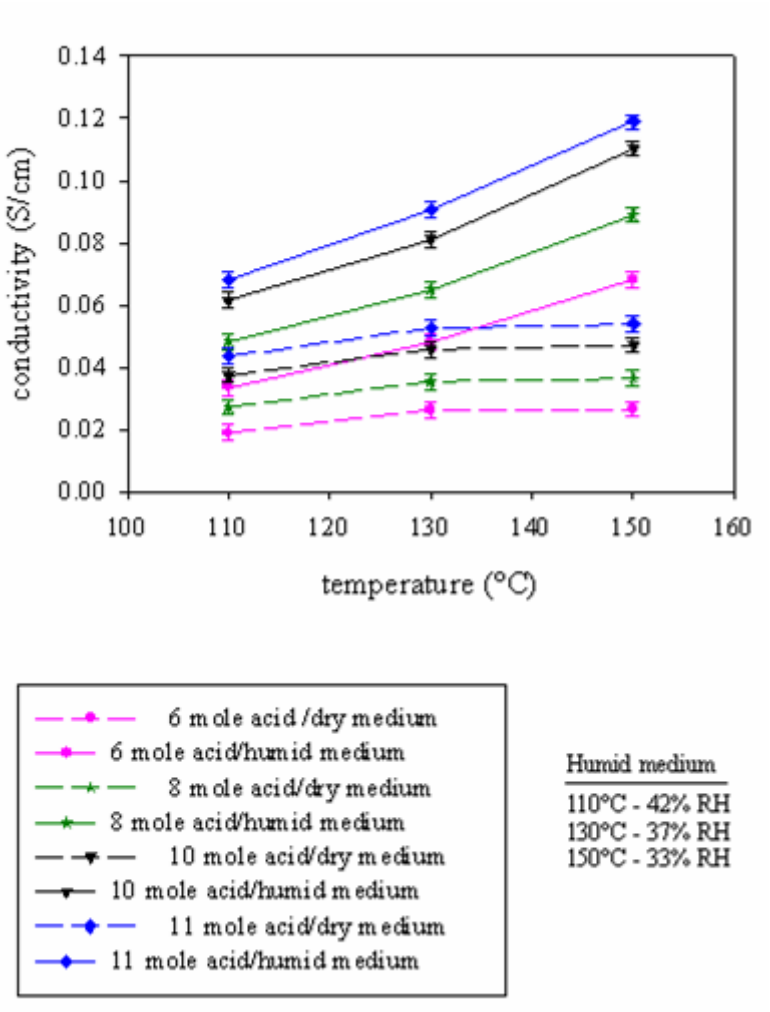

Figure 23. The conductivity data for the acid doped mPBI membranes prepared

decreased with increasing temperature [27]. It means that smaller volume is enough for proton transfer through the membrane as temperature is increased which results in lower resistance to the proton transfer.

The measurements showed that conductivity levels comparable with Nafion® (>0.1 S/cm) could be obtained at high temperatures when the acid doping level was increased to 10-11 mole. It means that these membranes enable PEMFC's to operate at high temperatures (up to 200°C) with sufficient performance, so that the advantages of operation at high temperatures such as higher tolerance of Pt catalyst to impurities, enhanced reaction kinetics and mass transport, and easier water and heat management in the PEMFC would be taken using the mPBI/H_3PO_4.

During the conductivity measurements, the membranes remained mechanically stable. After the measurements, the membranes were checked for any degradation, and it was not observed any degradation for them due to the high molecular weight of polymer used in the membrane preparation. Therefore, there was no need to determine an optimum value of acid doping level. The membrane having the highest acid doping level and conductivity value (that having 11 moles of doped acid), can be recommended for the PEMFC operation at 150°C. The humidity level would be lower than 33% RH to eliminate the requirement of pressurizing the system.

The conductivity of the membrane having an acid doping level of 6 moles at 18°C and 45% RH was measured as 3.1×10^{-4} S/cm which was indeed very low. This showed that these membranes were only suitable at high temperatures.

To determine the reliability of the humidity chamber, the conductivity of Nafion 112 was measured at 80°C and 100% RH. It was found as 0.11 S/cm which was consistent. Therefore, it can be said that the conductivity values of mPBI membrane obtained in this study were reliable enough to make conclusions.

The conductivity measurements in dry air were performed at atmospheric pressure. However, those in humid medium were not performed at constant pressure, and it varied as the temperature inside the chamber was changed (from 110°C to 150°C → from 0.6 bar to 1.6 bar as indicated in Table 5). Actually, the changes in pressure were not high enough to affect the conductivity level. A study

indicated that a pressure change of 500 bar affected the conductivity by 1-2 % [47], and so it can be said that even these levels of pressure change had a negligible effect on conductivity.

Table 5. The pressure readings from the manometer during the experiments at different temperatures and the RH values according to these readings

temperature (°C)	110	130	150
reading (bar)	0.60	1.00	1.60
P_v (bar)	0.60	1.00	1.60
P_{sat} (bar) [49]	1.43	2.70	4.76
RH%	42	37	33

CHAPTER 5

CONCLUSIONS

This study was a part of a research for development of PEM fuel cells operating high temperature. The study was conducted to prepare phosphoric acid doped polybenzimidazole membranes for high temperature (>100°C) PEM fuel cells. For this purpose, the poly [2,2'-(m-phenylene)-5,5'-bibenzimidazole], which is one of the aromatic polybenzimidazoles with high mechanical strength, thermal and oxidative stability, was synthesized; then several membranes with different acid doping levels were prepared from the synthesized polymer for the characterization.

The polymer was synthesized by using the method of polyphophoric acid solution polymerization. To synthesize polymers having high molecular weight, two of the reaction parameters, the reaction time and the stirring rate, were investigated and optimized. 17 hrs of reaction time at 200°C was found to be enough for completion of polymerization. 300 rpm of stirring rate of reaction solution resulted in synthesizing polymers with higher molecular weights compared to those synthesized with a stirring rate of 1000 rpm.

The synthesized polymer was characterized by the analysis of infrared spectra, X-Ray powder diffraction, NMR spectra, and thermogravimetric analysis. The infrared spectra included five sharp peaks at 1620, 1528, 1438, 1280 and 796 cm^{-1}. The X-Ray data of polymer had only one peak, which was a wide one, at 2θ = 25°, indicating the linearity and amorphism of polymer. NMR data included a peak at 13.3 ppm which was the indication of proton of imidazole ring, and peaks between 7.65 and 9.15 ppm which were due to the proton signal of phenyl groups. Thermogravimetric analysis in air with a temperature ramp of 5°C/min showed that the polymer had a decomposition temperature at around 450°C. The intrinsic viscosity was found via a dilute solution viscosity technique using sulphuric acid as solvent and an Ubbelohde type viscometer. The highest intrinsic viscosity was

found as 2.1 dl/g at 30°C. The average molecular weight was calculated by using the Mark-Houwink equation, and found as 126,000.

The membranes from the synthesized polymer were prepared by a solution casting method using DMAc/LiCl as solvent system, which is the most widely used method for the preparation of PBI membrane in the literature. 5 wt % of polymer was dissolved completely in DMAc/1wt % LiCl for max 2 hrs at 70°C using an ultrasonic bath.

Phosphoric acid solutions having four different concentrations, 11, 13, 14 and 14.7 M, were prepared, and the mPBI membranes cast from DMAc/ LiCl/mPBI solution were immersed into these solutions to dope them with acid. The resulting acid doping levels obtained were 6, 8, 10 and 11 molecules H_3PO_4/ mPBI repeat unit. The smallest thickness for the doped membranes was obtained as 60 μm.

The characterization of the doped membranes was performed by thermo-gravimetric analysis, mechanical tests and conductivity measurements. Thermo-gravimetric analysis was made in air in two stages: first the temperature was increased with a ramp of 2°C/min, and then the weight loss was recorded at uniform temperature of 200°C for 2 hrs. This analysis showed that two significant weight losses occurred: the first one was at 35-100°C due to the loss of free water in the membrane, the latter was at 120-200°C due to loss of water produced by dehydration of phosphoric acid molecules in the membrane. However, in a study, it was indicated that the weight loss was a reversible process at which the membrane could regain its weight at lower temperatures (i.e. 110°C) in humid medium. Therefore, it was concluded from the TGA data that the acid doped mPBI membranes had no permanent weight loss and so no decomposition point up to 200°C. The tension tests of the membranes having η_{int} = 2.1 dl/g with different acid doping levels were performed at ambient conditions. The highest stress value was obtained as 23 MPa for the membrane at a doping level of 6 moles, and the lowest one was measured as 11 MPa for 11 mole of acid doping. The conductivity measurements were performed using the technique of four probe impedance spectrum for the membranes with doping levels of 6, 8, 10 and 11 mole at three different temperatures, 110, 130 and 150°C, in both dry and humid air. Different

humidity levels at high temperatures were obtained in a humidity chamber: 110°C – 42% RH, 130°C – 37% RH, 150°C – 33% RH. The impedance analysis was performed using a potentiostat, and according to the impedance data obtained, the highest conductivity was found as 0.12 S/cm for the membrane having 11 moles of acid doping level at 150°C and 33% RH. The conductivity was calculated as 0.07 S/cm for the membrane with a doping level of 6 moles at 150°C and 33 RH, which is the most analyzed membrane for conductivity measurements in literature. This value is also plausible Acceptable conductivity levels were also obtained in dry air. The membrane having an acid doping level of 11 moles had a conductivity value of 0.05 S/cm at 150°C in dry air, which was a promising result for using mPBI membranes in PEMFC's without humidification.

In conclusion, phosphoric acid doped polybenzimidazole membranes were prepared for PEM fuel cell tests by this study. The polybenzimidazole polymer with high molecular weight was synthesized, so that it was possible to dope the polymer membranes with high levels of acid without the limitation of mechanical strength. High conductivity levels were obtained comparable with that of Nafion® for the membranes with high doping levels.

CHAPTER 6

RECOMMENDATIONS

In this study, the mPBI polymer was synthesized and acid doped membranes were prepared from this polymer. The measurements of ionic conductivity indicated that the mPBI was a promising alternate for the PEMFC operation even at dry conditions. The next step would be the development of MEA preparation methods for the mPBI membrane, and performing the fuel cell tests with the MEA's to be prepared. The optimum operating conditions for the PEMFC would be determined by observing the effect of temperature, pressure, humidity and acid doping level. The life-time tests would be performed, and the reasons for degradation would be investigated.

The mPBI membrane is susceptible to acid leaching. To prevent the loss of free acid during operation which results in decrease in fuel cell performance, morphological changes in polymer structure would be made. Some side chains to which extra acid molecules could be bonded would be added into the phenyl groups of the mPBI polymer. Blends with other polymers such as sPEEK, sPEK and sPES would be prepared.

REFERENCES

1. L. Masters, M. Gilbert, *Renewable and Efficient Electric Power Systems*, J. Wiley & Sons Inc., 2004

2. W. R. Grove, "On voltaic series and the combination of gases with platinum" *Philosophical Magazine*, vol. 14, p. 127, 1839

3. W. R. Grove, "On the gas voltaic battery: Experiments made with a view of an ascertaining the rationale of its action and its application to eudiometry", *Philosophical Transactions of the Royal Society of London*, vol. 133, p. 91, 1843

4. L. Mond, C. Langer, "A new form of gas battery", *Proceedings of the Royal Society of London*, vol. 46, p. 296, 1889

5. Encyclopedia Britannica Online -Academic Edition-, *Development of fuel cells*, http://search.eb.com/eb/article-45868, 26th Feb. 2007

6. F. Barbir, *PEM Fuel Cells Theory and Practice*, Elsevier Academic Press, 2005

7. C. C. Sorrell, *Materials for Energy Conversion Devices*, Woodhead Publishing Ltd., 2005

8. Fuel Cells- "A 21st century power system", *Journal of Power Sources*, vol. 71, p. 12, 1998

9. A. B. Staumbouli, E. Traversa, "Fuel cells, an alternative to standard sources of energy", *Renewable and Sustainable Energy Reviews*, vol. 6, p. 297, 2002

10. G. J. K. Acres, "Recent advances in fuel cell technology and its applications", *Journal of Power Sources*, vol. 100, p. 60, 2001

11. J. S. Wainright, J.-T. Wang, D. Weng, R. F. Savinell, M. Litt, "Acid doped polybenzimidazoles: A new polymer electrolyte", *Journal of Electrochemical Society*, vol. 142, p. L121, 1995

12. R. B. Bird, W. E. Stewart, E. N. Lightfoot, *Transport Phenomena*, J. Wiley &Sons Inc., 2001

13. J. Zhang, Z. Xie, J. Zhang, Y. Tang, C. Song, T. Navessin, Z. Shi, D. Song, H: Wang, D. P. Wilkinson, Z. S. Liu, S. Holdcroft, "High temperature PEM fuel cells", *Journal of Power Sources*, vol. 160, p. 872, 2006

14. B. R. Einsla, "High temperature polymers for proton exchange membrane fuel cells", *Ph. D. Dissertation*, Virginia Polytechnique Institute and State University, VA, USA, April 2005

15. O. Savadogo, "Emerging membranes for electrochemical systems part II. high temperature composite membranes for polymer electrolyte fuel cell (PEFC) applications, *Journal of Power Sources*, vol. 127, p. 135, 2004

16. Q. Li, R. He, J. O. Jensen, N. J. Bjerrum, "Approaches and recent development of polymer electrolyte membranes for fuel cells operating above 100 °C", *Chemistry of Materials*, vol. 15, p. 4896, 2003

17. G. Inzelt, M. Pineri, J. W. Schultze, M. A. Vorotyntsev, "Electron and proton conducting polymers: recent developments and prospects", *Electrochimica Acta*, vol. 45, p. 2403, 2000

18. J. A. Kerres, "Development of ionomer membranes for fuel cells", *Journal of Membrane Science*, vol. 185, p. 3, 2001

19. B. Smitha, S. Sridhar, A. A. Khan, "Solid polymer electrolyte membranes for fuel cell applications- a review", *Journal of Membrane Science*, vol. 259, p. 10, 2005

20. Q. Li, R. He, J. O. Jensen, N. J. Bjerrum, "PBI-based polymer membranes for high temperature fuel cells-preperation, characterization and fuel cell application", *Fuel Cells*, vol. 4, p. 147, 2004

21. K. C. Brinker, I. M. Robinson, "Poly(N-arylenebenzimidazole)s via aromatic nucleophilic displacement", *US Patent: 2,895,948*, 1959

22. H. Vogel, C. S. Marvel, "Polybenzimidazoles, new thermally stable polymers", *Journal of Polymer Science*, vol. L, p. 511, 1961

23. H. F. Mark, N. G. Gaylord, N. M. Bikales, *Encyclopedia of Polymer Science and Technology*, vol. 11, Wiley-Interscience, 1969

24. J. C. Salamone, *Polymeric Materials Encyclopedia*, vol. 7, CRC Press Inc., 1996

25. E-W. Choe, "Catalysts for the preparation of polybenzimidazoles", *Journal of Applied Polymer Science*, vol. 53, p. 497, 1994

26. Y. Iwakura, K. Uno, Y. Imal, “Polyphenylenebenzimidazoles”, *Journal of Polymer Science: Part A*, vol. 2, p. 2605, 1964

27. H. Zang, “Novel phosphoric acid doped polybenzimidazole membranes for fuel cells”, *Ph. D. Dissertation*, Rensselaer Polytechnique, NY, USA, December 2004

28. Y. Iwakura, K. Uno, Y. Imai, “Process for preparation of polybenzimidazoles”, *United State Patent*, no. 3,313,783, 1963

29. R. He, Q. Li, A. Bach, J. O. Jensen, N. J. Bjerrum, “Physicochemical properties of phosphoric acid doped polybenzimidazole membranes for fuel cells”, *Journal of Membrane Science*, p. 6910, 2005

30. L. Xiao, H. Zhang, E. Scanlon, L. S. Ramanathan, E.-W. Choe, D. Rogers, T. Apple, B. C. Benicewicz, “High temperature polybenzimidazole fuel cell membranes via a sol-gel process”, *Chemistry of Materials*, vol. 17, p. 5328, 2005

31. J. Lobato, P. Canizares, M. A. Rodrigo, J. J. Linares, G. Manjavacas, “Synthesis and characterization of poly[2,2’-m-(phenylene)-5,5’-benzimidazole] as polymer electrolyte membrane for high temperature PEMFC’s”, *Journal of Membrane Science*, vol. 280, p. 351, 2006

32. L. Qingfeng, H. A. Hjuler, N. J. Bjerrum, “Phosphoric acid doped polybenzimidazole membranes: Physicochemical characterization and fuel cell applications”, *Journal of Applied Electrochemistry*, vol. 31, p. 773, 2001

33. O. E. Kongstein, T. Berning, B. Borresen, F. Seland, R. Tunold, “Polymer electrolyte fuel cells based on phosphoric acid doped polybenzimidazole (PBI) membranes”, *Energy*, vol. 32, p. 418, 2007

34. M. Litt, R. Ameri, Y. Wang, R. Savinell, J. S. Wainright, “Polybenzimidazoles/ phosphoric acid solid polymer electrolytes: mechanical and electrical properties” *Material Research Society Symposium Proceedings*, vol. 548, p. 313, 1999

35. R. Ameri, “Polybenzimidazole Film Containing Acid as Proton Exchange Membrane (PEM)”, *Ph. D. Dissertation*, Case Western Reserve University, Ohio, USA, 1997

36. C. B. Shogbon, J.- L. Brousseau, H. Zhang, B. C. Benicewicz, Y. A. Akpalu, “Determination of the Molecular Parameters and Studies of the Chain Conformation of Polybenzimidazole in DMAc/LiCl”, *Macromolecules*, vol. 39, p. 9409, 2006

37. Q. Li, R. He, R. W. Berg, H. A. Hjuler, N. J. Bjerrum, “Water uptake and acid doping of polybenzimidazoles as electrolyte membranes for fuel cells”, *Solid State Ionics*, vol. 168, p. 177, 2004

38. S. R. Samms, S. Wasmus, R. F. Savinell, “Thermal Stability of Proton Conducting Acid Doped Polybenzimidazole in Simulated Fuel Cell Environments”, *Journal of Electrochemical Society*, vol. 143, p. 1225, 1996

39. M. Kawahara, J. Morita, M. Rikukawa, K. Sanui, N. Ogata, “Synthesis and proton conductivity of thermally stable polymer electrolyte: poly(benzimidazole) complexes with strong acid molecules”, *Electrochimica Acta*, vol. 45, p. 1395, 2000

40. D. Weng, J. S. Wainright, U. Landau, R. F. Savinell, “Electro-osmotic drag coefficient of water and methanol in polymer electrolytes at elevated temperatures”, *Journal of Electrochemical Society*, vol. 143, p. 1260, 1996

41. Y.-L. Ma, J. S. Wainright, M. H. Litt, R. F. Savinell, “Conductivity of PBI membranes for high-temperature polymer electrolyte fuel cells”, *Journal of Electrochemical Society*, vol. 151, p. A8, 2004

42. D. J. Jones, J. Roziere, “Recent advances in functionalisation of polybenzimidazole and polyetherketone for fuel cell applications”, *Journal of Membrane Science*, vol. 185, p. 41, 2001

43. A. Buckley, D. Stuetz, G. A. Serad, “Polybenzimidazoles”, *Encyclopedia of Polymer Science and Engineering*, p. 572, Wiley, 1987

44. A. Carollo, E. Quartarone, C. Tomasi, P. Mustarelli, F. Belotti, A. Magistris, F. Maestroni, M. Parachini, L. Garlaschelli, P. P. Righetti, “Developments of new proton conducting membranes based on different polybenzimidazole structures for fuel cell applications”, *Journal of Power Sources*, vol. 160, p. 175, 2006

45. A. Sannigrahi, D. Arunbabu, R. M. Sankar, T. Jan, “Aggregation Behavior of Polybenzimidazole in Aprotic Polar Solvent”, *Macromolecules*, vol. 40, p. 2844, 2007

46. A. Ainla, D. Brandell, “Nafion®–polybenzimidazole (PBI) composite membranes for DMFC applications”, *Solid State Ionics*, vol. 178, p. 581, 2007

47. R. Bouchet, S. Miller, M. Duclot, J. L. Souquet, “A thermodynamic approach to proton conductivity in acid-doped polybenzimidazole”, *Solid State Ionics*, vol. 145, p. 69, 2001

48. J. Branrup, E. H. Immergut, *Polymer Handbook*, Wily-Intersience, Wiley-Intersicence, 1989

49. S. I. Sandler, *Chemical and Engineering Thermodynamics*, J. Wiley&Sons, 1999

APPENDIX A: PROPERTIES OF FUEL CELL TYPES

Table 6. Types of FC's and their properties

	PAFC	**MCFC**	**SOFC**	**AFC**	**PEMFC**
T_{op}	170-200	600-700	900-1000	50-200	60-80
Fuel	H_2 (CO<2%)	H_2, CO	H_2, CO, CH_4	H_2	H_2 (CO<50ppm)
Electrolyte	H_3PO_4	Li_2CO_3, Na_2CO_3	ZrO_2, Y_2O_3	KOH	proton exchange polymer
Transferred ion	H^+	CO_3^{-2}	O^{-2}	OH^-	H^+
Anode catalyst	Pt/C	Ni	Ni	Ni, Pt/Pd	Pt/C, Pt-Ru/C
Cathode catalyst	Pt/C	NiO	LaSr, MnO_3	Ag, NiO, Au/Pt	Pt/C, Pt-Fe/C
Electrical efficiency	40-45	45-60	50-60	60	40-50
Possible applications	Power stations	Power stations	Power stations	Submarines Spacecrafts	Vehicles, Portables, Stationary

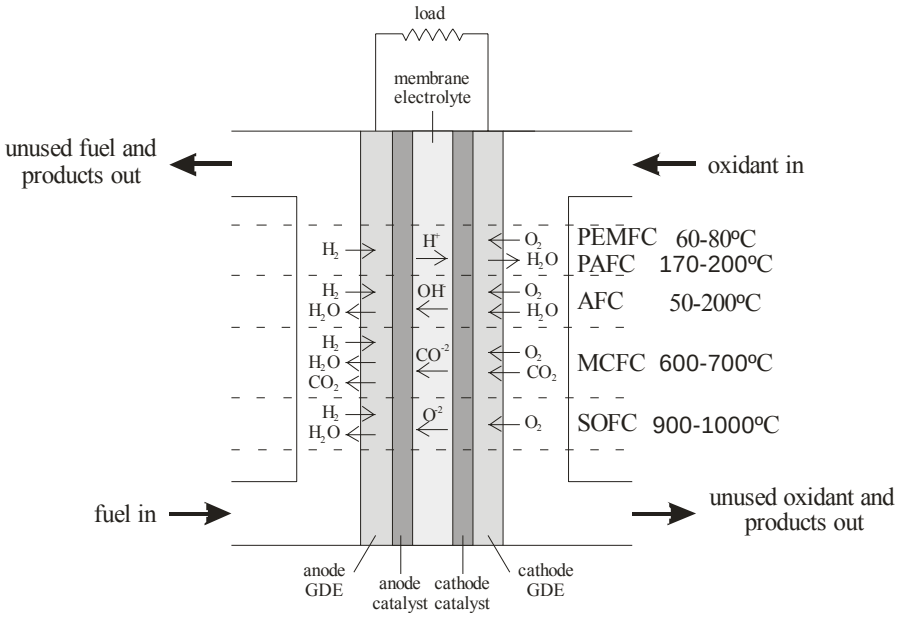

Figure 24. Types of FC's with their reactions and T_{op}'s [6]

APPENDIX B: SOME EXPERIMENTAL DATA FOR ACID DOPED PBI MEMBRANES

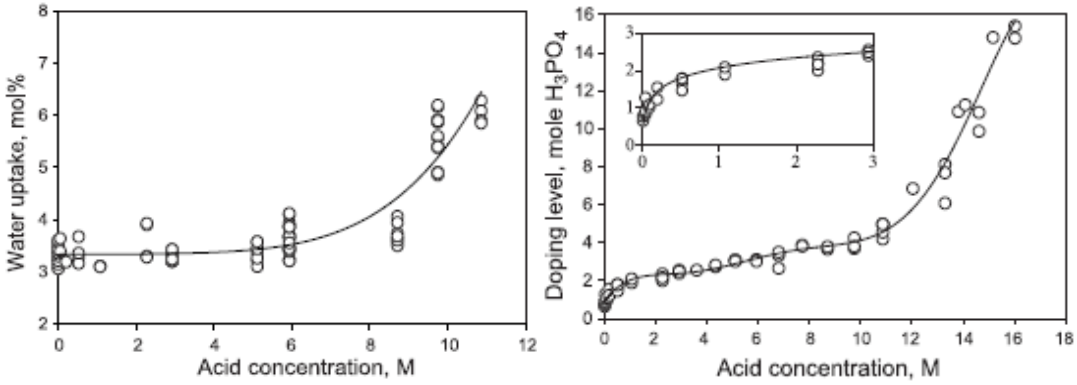

a b

Figure 25. Water uptake (a) and acid doping level (b) of mPBI membrane in different acid concentrations at room temperature [37]

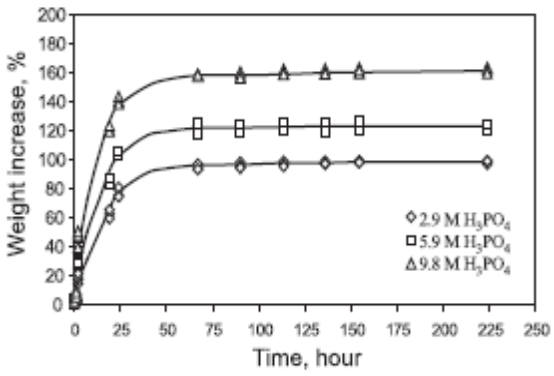

Figure 26. Weight increase of mPBI membrane after immersing into acid solution at room temp. [37]

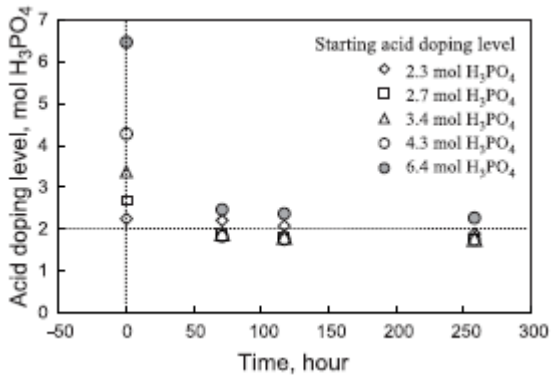

Figure 27. Residual amount of acid in mPBI membrane after immersing the membrane samples in methanol [37]

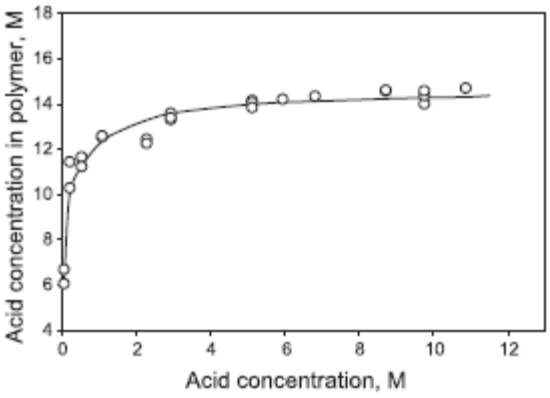

Figure 28. Concentration of the acid inside mPBI membranes as a function of the acid solution [37]

APPENDIX C: PROTON TRANSFER MECHANISM THROUGH PBI MEMBRANE

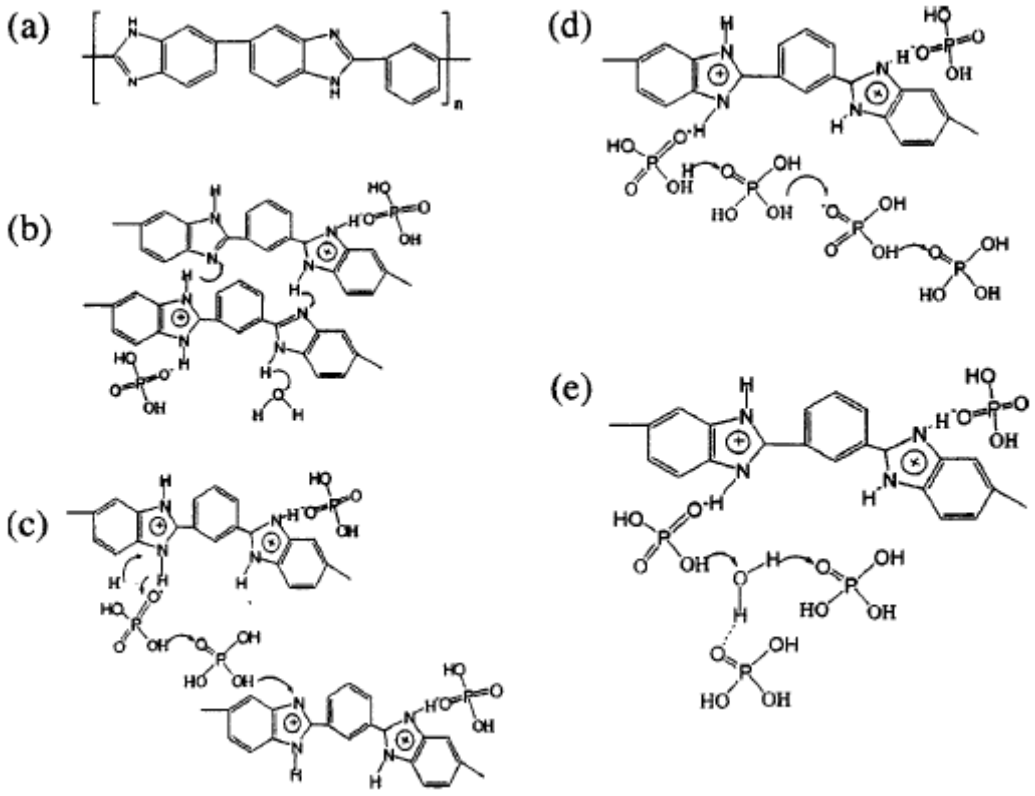

Figure 29. Chemical structure of (a) mPBI, (b) H_3PO_4 protonated mPBI, (c) proton transfer along acid-BI-acid, (d) proton transfer along acid-acid, (e) proton transfer along acid-H_2O [41]

APPENDIX D: HUMIDITY CALCULATION

The humidity at high temperatures is supplied by pumping a measured amount of water to the humidity chamber. Because the air inside the chamber is evacuated before sending water into the system, the pressure read from the manometer at a temperature corresponded to that of water vapor only. According to Dalton's law of partial pressures, the total pressure for the water vapor + air system can be written in terms of the partial pressures of water vapor and air as shown in Equation (F.1),

$$P_T = P_v + P_{air} \quad \text{(F.1)}$$

where P_T: total pressure in the chamber which is read from the manometer

P_v: partial pressure of water vapor in the chamber

P_{air}: partial pressure of dry air in the chamber

In this equation, the term, P_{air} is equal to zero for the system, so P_T is equal to P_v. The RH is expressed in terms P_v and saturation pressure (P_{sat}) at the temperature at which the pressure reading is made, as in Equation (F.2),

$$RH\% = \frac{P_v}{P_{sat}} x100 \quad \text{(F.2)}$$

The pressure readings from the manometer during the experiments, and the RH values calculated using Equation (F.2) are given in Table 5.

APPENDIX E: CALCULATION OF VISCOSITY

The flow times, t, measured by the Ubbelohde viscometer were used for the calculation of η_{int}. They are related to the viscosity of the solution (η) by an equation of the form indicated in Equation (G.1) [48],

$$\frac{\eta}{\rho} = \nu = at - \frac{b}{t} \qquad \text{(G.1)}$$

where η: viscosity

υ: kinematic viscosity

a, b: instrument constants

The last term in Equation (G.1) is the term of kinetic energy correction, and it is negligible for flow times over a minute. Besides, the densities of the dilute polymer solutions differ little from that of the solvent. Therefore, the proportion of the viscosities of the solution and solvent can be expressed as indicated in Equation (G.2),

$$\frac{\eta}{\eta_0} = \frac{t}{t_0} \qquad \text{(G.2)}$$

where η_0: viscosity of the solvent

Actually, there are two methods for calculating η_{int}. In the first method, the specific viscosity (η_{sp}) for four different concentrations at which the flow times, t, are recorded is calculated by the Equation (G.3),

$$\eta_{sp} = \frac{\eta - \eta_0}{\eta_0} = \frac{t - t_0}{t_0} \qquad \text{(G.3)}$$

Then, the reduced viscosity (η_{red}) is found by the Equation (G.4),

$$\eta_{red} = \eta_{sp} / c \qquad \text{(G.4)}$$

where c: concentration level in the viscometer (g/dl)

After that, η_{red} vs. c is plotted. Because mPBI is a linear molecule, this plot should give a straight line. A linear equation in the form of y = ax + b is fitted to this plot.

The value of b gives η_{int}, which is related to the definition of η_{int} as given in Equation (G.5),

$$\eta_{int} = \lim_{c \to 0} (\eta_{red}) \qquad \text{(G.5)}$$

In the second method, the relative viscosity (η_{rel}) for four different concentrations, at which the flow times, t, are recorded is calculated by the Equation (G.6),

$$\eta_{rel} = \frac{\eta}{\eta_0} = \frac{t}{t_0} \qquad \text{(G.6)}$$

Then, the inherent viscosity (η_{inh}) is found by the Equation (G.7),

$$\eta_{inh} = \ln(\eta_{rel}) / c \qquad \text{(G.7)}$$

After that, η_{inh} vs. c is plotted. This plot also gives a straight line. A linear equation in the form of y = ax + b is fitted to this plot. The value of b gives η_{int}, which is related to another definition of η_{int} as given in Equation (G.8),

$$\eta_{int} = \lim_{c \to 0} (\eta_{inh}) \qquad \text{(G.8)}$$

As an example, the calculation of η_{int} for the fifth synthesis the reaction conditions of which are given in Table 2 can be indicated as follows: t_0 for the pure sulphuric acid solution at 30°C was found as 1.56 min. At the solution concentrations of 0.4, 0.6, 0.8 and 1.0 g/dl, t were measured as 4.08, 5.38, 7.23 and 9.34 min.

By using the first method, η_{sp} and η_{red} were calculated for each concentration level using Equation (G.3) and (G.4), respectively. Those for the concentration of 0.4g/dl is calculated below as an example,

$$\eta_{sp} = \frac{t - t_0}{t_0} = \frac{248 - 116}{116} = 1.14$$

$$\eta_{red} = \eta_{sp} / c = \frac{1.14}{0.4 gr/dl} = 2.84 \text{ dl/g}$$

This was repeated for the remaining concentrations (The values are tabulated in Table 7.). Thereafter, the four values of η_{red} vs. c were plotted as indicated in Figure 30. A linear curve was also fitted to the plot, and the intersection of this curve with

Y-axis, which gave the value of η_{int} for the analyzed mPBI. The intersection point and so η_{int} is approximately 2.1 dl/g.

This value can be also found by using the second method. As an example, η_{rel} and η_{inh} are calculated for the concentration of 0.4g/dl,

$$\eta_{rel} = \frac{t}{t_0} = \frac{248}{116} = 2.14$$

$\eta_{inh} = \ln(\eta_{rel}) / c = \ln(2.14)/0.4g/dl = 1.90$ dl/gr

This was repeated for the remaining concentrations (The values are tabulated in Table 7.) Thereafter, the four values of η_{red} vs. c were plotted as indicated in Figure 30. A linear curve was also fitted to the plot, and the intersection of this curve with Y-axis, which gave the value of η_{int} for the analyzed mPBI. The intersection point and so η_{int} is approximately 2.1 dl/g. This is same with that obtained by the first method.

Table 7. The measured flow times and the calculated viscosities for mPBI from fifth synthesis

Concentration (g/dl)	**0.4**	**0.6**	**0.8**	**1.0**
t_0 (s)	116	116	116	116
t (s)	248	338	443	574
η_{sp} (dimensionless)	1.14	1.91	2.82	3.95
η_{red} (dl/g)	2.84	3.19	3.52	3.95
η_{rel}	2.14	2.91	3.82	4.95
η_{inh}	1.90	1.78	1.67	1.60

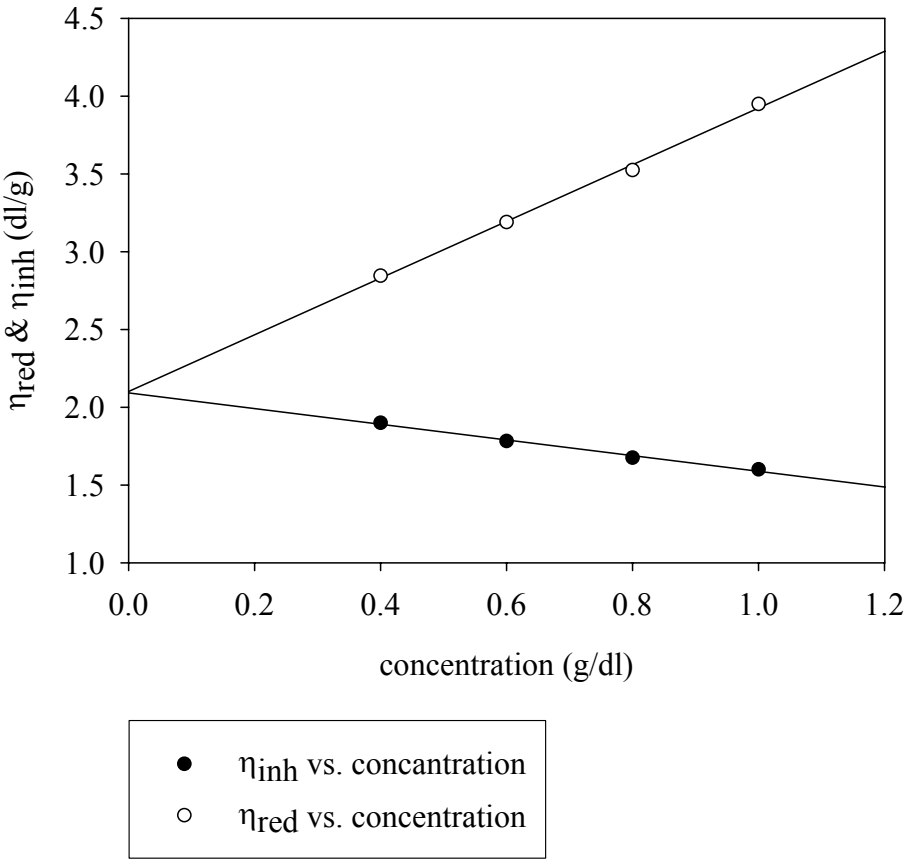

Figure 30. The plot of η_{red} vs. c for the mPBI from synthesis 5

APPENDIX F: DESCRIPTION OF INFRARED SPECTRA OF PBI POLYMER

Table 8. The description of the spectra of mPBI [23]

Wave number (cm^{-1})	Wavelength (μ)	remarks
3400 (weak)	2.94	N-H
3000-3200 (strong, broad)	3.33-3.13	C-H
2910 (medium)	3.44	
1612 (strong)	6.4	C=C, C=N
1590 (medium)	6.29	conjucation between benzene and imidazole rings
1528 (medium, sharp)	6.55	characteristic of 2-substitution
1548 (medium)	6.89	characteristic of substituted benzimidazole, in-plane vibration
1438 (sharp)	6.98	characteristic of substituted benzimidazole, in-plane vibration
1410 (medium, sharp)	7.1	C-C stretch
1398 (medium, sharp)	7.18	
1280 (medium)	7.8	C-N stretch
1226	8.18	characteristic of 2- and 5-substitution
1167 (weak)	8.6	characteristic of benzimidazoles
1094 (weak)	9.13	characteristic of 2-substitution
1011 (medium)	9.89	benzene ring vibration
980 (medium)	10.21	benzene ring vibration
950 (medium)	10.52	
898 (medium)	11.15	Heterocyclic ring vibration
840 (medium)	11.9	two adjacent hydrogens in six-membered ring (C-H out-of-plane bend)
796 (sharp)	12.59	three adjacent hydrogens in six-membered ring (C-H out-of-plane bend)
756 (weak)	13.21	Heterocyclic ring vibration
705 (medium, sharp)	14.2	2-substituted benzimidazole
690 (medium)	14.5	3,4-disubstituted biphenyl, C-H out of place
655 (weak)	15.28	
600 (weak)	16.68	
596 (weak)	16.8	

APPENDIX G: X-RAY DATA OF PBI

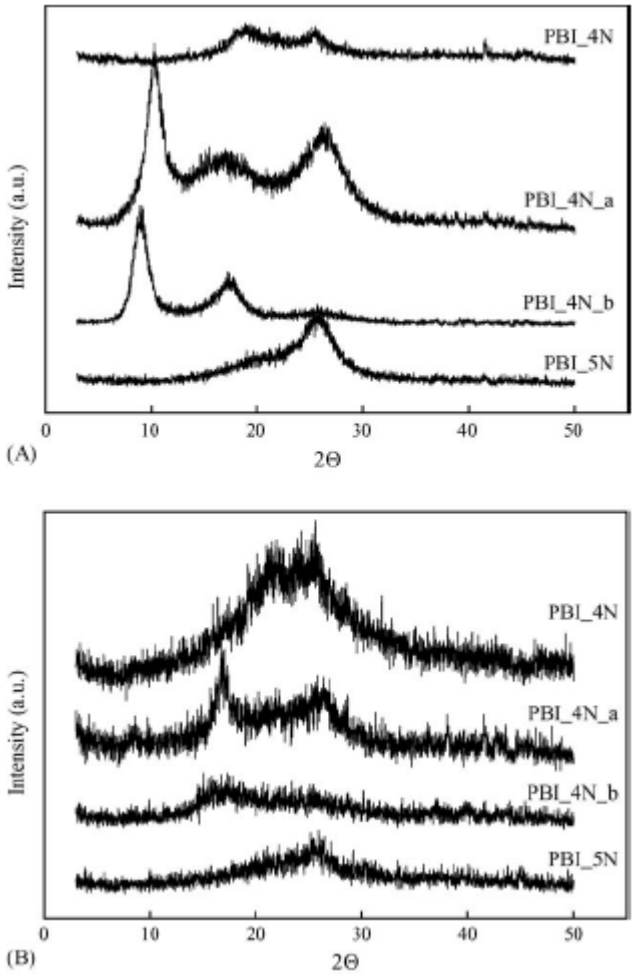

Figure 31. X-Ray diffraction patterns of undoped (A) and doped (B) PBI films (PBI_4N means mPBI in the graphs.) [44]